Chinese Chemical Letters 34 (2023) 107670

Contents lists available at ScienceDirect

Chinese Chemical Letters

journal homepage: www.elsevier.com/locate/cclet

Advances in application of sensors for determination of phthalate esters

Chuanxiang Zhang[a], Jie Zhou[b], Tingting Ma[b], Wenfei Guo[b], Dan Wei[b], Yimin Tan[a,*], Yan Deng[b,*]

[a] College of Packing and Materials Engineering, Hunan University of Technology, Zhuzhou 412007, China
[b] Hunan Key Laboratory of Biomedical Nanomaterials and Devices, Hunan University of Technology, Zhuzhou 412007, China

ARTICLE INFO

Article history:
Received 3 April 2022
Revised 7 July 2022
Accepted 8 July 2022
Available online 9 July 2022

Keywords:
Phthalate esters
Sensors
Electrochemical
Optical
Determination

ABSTRACT

Phthalates esters (PAEs) are extensively used as additives for polymers in plastic, particularly in polyvinyl chloride (PVC) and polyethylene terephthalate (PET). These compounds are not part of the polymer chains and can be released easily from products and migrate into beverages and foods that come into direct contact, causing environmental and human health impacts. Simple and rapid detection of such substances is of great significance for ensuring environmental food safety and consumer health. At present, optical sensor and electrochemical sensor detection technologies have been applied to PAEs detection due to their advantages, such as simple, rapid, low cost, high sensitivity, simple operation, portability and high specificity. They can make up for the shortcomings of chromatographic detection technology, such as expensive equipment, cumbersome operation, the need for professional and technical personnel, and difficulty in achieving a large number of sample screening objectives. In this paper, research progress on optical sensors and electrochemical sensors for the detection of phthalates in recent ten years is reviewed and discussed. This is helpful to better understand preparation methods for sensors and their detection mechanisms for phthalates. The review will also be used in developing a more effective trace detection sensor for phthalates.

1. Introduction

Phthalates esters (PAEs) are a group of chemical compounds, which include dialkyl or alkyl aryl esters of 1,2-benzenedicarboxylic acid. The different number of carbon atoms in alkyl groups endows them with various physical and chemical properties [1]. Some of these compounds, such as dibutyl phthalate (DBP), diethyl hexyl phthalate (DEHP), dioctyl phthalate (DOP), diisononyl *ortho*-phthalate (DINP) and butyl benzyl phthalate (BBP), are widely used legally or illegally as plasticizer, softener and additive [2,3] in hundreds of products such as toys [4], food packaging materials [5,6], medical blood bags [7] hoses [8], cleaning agents [9], lubricants [10], personal care items [9,11], and other countless commercial [12] and agricultural applications [13], due to their excellent performance and low synthesis cost. Nevertheless, although PAEs are the main components of plasticizers, they are not chemically bonded to plastic components, which relies on hydrogen bonds or van der Waals forces to bind to plastic molecules. These forces are weak, so under certain conditions they are constantly released into the surrounding environment across all stages of the product life cycle, causing pollution [9,14,15]. Numerous studies have shown that PAEs are commonly found in soil, atmosphere, water, organisms and even human body and other natural and human environments [16]. At present, phthalate ester pollutants have been detected in the atmosphere [15], seawater [17], groundwater [18,19], surface water [20], drinking water [21,22], soil [23], sediments [24,25], biota [26], vegetables [27], milk and so on. More than 20 PAEs congeners have been detected in the environment [28,29]. Moreover, to take advantage of PAEs, some illegal food businesses tend to even add PAEs into food products to replace expensive additives, causing serious harm to consumers. And these lipophilic compounds can enter the human body through numerous ways, such as food intake, breathing, skin contact, and bioaccumulate in the human body [30–32]. A growing body of evidence suggests that after being absorbed, PAEs are mainly distributed

* Corresponding authors.
E-mail addresses: csfutanyimin@126.com (Y. Tan), hndengyan@126.com (Y. Deng).

https://doi.org/10.1016/j.cclet.2022.07.013
1001-8417/

in various organs of the body in the form of protein complexes through the bloodstream, causing chronic toxic effects and even affecting human respiratory system function [33], reproductive development function [34–36] and thyroid function [22,37], as well as interfering with normal glucose and lipid metabolism, causing damage to human viscera. Animal toxicology studies showed that PAEs are the potential cause of numerous diseases, such as (1) mutagenic and carcinogenic [38–40], (2) child attention deficit disorder [41], (3) endocrine disorders [1,42], (4) fetal malformation [17], (5) kidney damage [43], (6) oligospermia and necrospermia [44,45], (7) decreased lung function, (8) and decreased rate of pregnancy [41]. The U.S. Environmental Protection Agency has listed PAEs as an environmental priority pollutant [46], and it is also called 'the second global polychlorinated biphenyls pollutant'. Phthalates are ubiquitous environmental pollutants due to their widespread production, use and disposal, as well as their high concentration in plastics and their ability to migrate from plastics [47]. The environmental pollution caused by phthalate esters has attracted global attention because of its wide range of application, large contaminated area, large number of people affected, and is more serious than that of metal and pesticide residues [48]. The maximum allowable limit for DEP, DBP, DMP, DEHP, in drinking water were set at 0.55, 0.45, 5.0 and 5.0 mg/L [49], respectively. Therefore, it is necessary to develop reliable and sensitive methods for determination of these trace compounds in a complex matrix. With advancement of techniques for trace analysis over the past decade, the determination technologies of phthalate esters are also gradually mature, with most commonly used methods for identification of phthalates and their metabolites being gas chromatography (GC) [43], high performance liquid chromatography (HPLC) [50], liquid chromatography and gas chromatography coupled with mass spectrometry (GC–MS) [42,51-54] or solid phase extraction [55,56], which have been considered as accurate, precise and robust methods. Nonetheless, these instrumental methodologies are time-consuming and expensive, and due to similar structure of various PAE homologues, complex instrument separation and detection conditions need to be explored, which increases the difficulty of analysis, and may also lead to experimental errors, hence requires professional technicians. Other methods, such as enzyme-linked immunosorbent assay (ELISA), have rarely been reported, and there are problems such as sample matrix interference and false positive easily. Therefore, the exploration of more simple, efficient, safe and cheap pretreatment methods or methods without pretreatment will be one of the focuses for future research. Such methods are electrochemical analytical method [57], optical analysis method [58,59] *etc*. Owing to their low-coat apparatus, high detection sensitivity, simple operation, portability and other advantages, these methods have been exploited as powerful analytical tools widely applied in environmental monitoring [60,61], food safety [62], drug analysis, clinical judgment and other fields [63–65].

During the last decade, the technologies for trace determination of phthalate esters have been rapidly developed. However, to the best of our knowledge, the reviews focused on optical and electrochemical detection of phthalate esters have rarely been presented. This paper therefore makes a summary and discussion on research progress on optical and electrochemical sensors for the detection of phthalate esters in recent years. This will contribute to a better understanding of preparation methods for sensors and their detection mechanisms, including development trend on phthalates sensing, and development of low cost, high accuracy and compatibility sensors for the trace detection of phthalates. The purpose is not only to provide guidance for the detection of phthalate esters, but also to provide reference for the development and progress of bisphenol, pesticides and antibiotics monitoring and other related research fields.

2. Sensors for determination of phthalate esters

As one of important means to obtain chemical or biological information, sensors can accurately and quickly identify and analyze specific targets, and convert them into available signals according to certain laws through physical, chemical, biological and other mechanisms, to achieve the purpose of detection [66–69]. With development of sensing technology and growing demand for sensors, the development of new, fast, convenient, high-throughput and real-time sensors has become one of the hot research fields [70–72]. In recent years, significant progress has been made in the development of electrochemical sensor and optical sensor detection of phthalates.

2.1. Electrochemical sensors for determination of PAEs

The electrochemical sensor is composed of a specific recognition element and a signal conversion unit. These specific identification elements react with the measured substance to produce an inductive signal, which is then converted by the inductive signal conversion unit into an identifiable electrical signal (*e.g.*, current, voltage, resistance) proportional to the concentration of the substance being measured. [73–75]. The measured substance is used as the sensitive source and the electrode as the conversion element. The development and innovation of electrochemical sensors emphasize on improving the quality of detection *via* improvement of selectivity and sensitivity of sensors [76–79]. The low electron transfer rate of the general working electrode is not enough to meet the practical application, so modifying the electrode of the sensor by utilizing different methods and materials individually or in combination is one of the main measures to improve the selectivity and sensitivity of the sensor. The selection of appropriate electrode modification materials is the guarantee that the electrochemical sensor can achieve accurate and reliable measurement [80–82]. The usage of nanomaterials (NMs) in electrode modification can improve the conductivity and electron transfer rate, while molecularly imprinted polymers and aptamers have higher selectivity and specificity to the substance to be detected [83–86]. In the following sections, the application of electrochemical sensors modified with nanomaterials, molecularly imprinted polymers and aptamers in the detection of phthalate plasticizers will be presented.

2.1.1. Electrochemical sensors based on nanomaterials for PAEs detection

The crucial element to obtain an electrochemical sensor with excellent performance and reliable quality is the type of material used for electrode modification. Nanomaterials have special properties different from macroscopic materials due to their small size and large specific surface area [87–94]. Compared to electrodes based on micro- or macro-materials, the usage of nanomaterials sensors takes advantage of increased electrode surface area, mass-transport rate, and fast electron transfer. Some response characteristics for the electrochemical sensor, such as selectivity, sensitivity are therefore improved by nanomaterials. Nanomaterials, especially modified nanomaterials, are increasingly applied in the manufacture of sensor materials [95,96]. With higher specific surface area, lower electron transport resistance and excellent ability to absorb chemical or biochemical substances, the modified nanosensors can be used for the detection of trace composition in different substrates, and even analytes that cannot easily be detected with conventional sensors. Therefore, the modification of nanosensors is of great value in the development and innovation of electrochemical analysis technology [97].

Metal nanomaterials especially noble metals nanomaterials, such as gold, silver, copper and platinum have excellent electrical conductivity, corrosion resistance, large specific surface area and

excellent catalytic performance [98,99], therefore, the modification of metal nanomaterials on the electrode surface is expected to reduce the over-potential for the reaction and accelerate the reaction rate for substance to be detected. Although most of these materials are expensive, their deposition on the surface of the sensor to form nanoparticles can greatly save the research cost and improve their utilization efficiency in EC sensors. Liu *et al.* [100] first developed an electrochemical immunosensor for the detection of dimethyl phthalate (DMP) utilizing platinum-lead (PtPb) hollow nanoparticles as signal labels. Platinum nanoparticles have large surface area, massive active sites, high catalytic performance, dramatic biocompatibility and excellent electrical conductivity. The introduction of Pb changes the crystal structure and electronic structure of Pt, improving the catalytic performance, and saving consumption of noble metals and reducing the cost. The electrochemical immunosensor fabricated by PtPb nanoparticles exhibits large linear response, low detection limit, distinct accuracy, high sensitivity and acceptable stability, showing infinite application potential for simple and rapid detection of DMP in actual samples. Gold nanoparticles, in particular, have high electron density and catalytic effect, simple chemical synthesis, excellent electrical conductivity, dramatic biocompatibility, narrow size distribution and other characteristics. Therefore, with development of nanoparticle detection technology, gold nanoparticles are considered as the most preferred electrode material used for sensing applications, which can be used to amplify electrochemical signals *via* steric-hindrance and electrostatic-repulsion. Zia *et al.* [101] used gold nanomaterials to modify silicon substrate to prepare planar inter-digital (ID) capacitive sensor, and quantified the presence of phthalates in ionic water and juice by EIS. Their results showed that the detection technology could rapidly and significantly detect the presence of DEHP in all test samples. However, unfortunately, if it is to be used in industrial applications, the selectivity of the sensor remains a challenge. Liang *et al.* [102] also developed a simple unlabeled electrochemical impedance immune sensor for the detection of dibutyl phthalate using the principle of signal induced amplification of gold nanoparticles. Here, NADH (nicotinamide adenine dinucleotide) is used as a nanoparticle catalytic growth reagent to obtain larger size of the AuNPs, thereby increasing the negative coating on the outer particles in the system. The corresponding electrochemical resistance increases, thus demonstrating the effectiveness of signal amplification. The prepared immunosensor exhibits dramatic comprehensive performance and can be widely used in the rapid and low-cost detection of DBP in a variety of samples. In recent years two-dimension (2D) transition metal dichalcogenides (TMDs) with the molecular formula of MX_2 (where M = Mo, W or Co and X = Se or S) have been also considered as a promising nanomaterial due to their fantastic physical and electronic properties. Of these, $CoSe_2$ can be considered the best because of its inherent metallic properties, which facilitate charge transfer efficiently. In reference [103], He *et al.* synthesized a $CoSe_2$ nanosheet material with fold and flake structure and large specific surface area by simple hydrothermal method. Then, the corrugation $CoSe_2$ (w-$CoSe_2$) was functionalized by polyethylene imine (PEI), and AuNCs/PEI-w-$CoSe_2$ nanocomposites were prepared by immobilization of gold nanocubes (AuNC) on the PEI-w-$CoSe_2$ surface *via* Au-N bond. The introduction of AuNCs/PEI-w-$CoSe_2$ nanocomposites improved the effective surface area and conductivity of the electrode, shown as Fig. 1. The prepared electrochemical immunosensor possess good specificity and rapid response for the detection of dipropyl phthalate (DPrP), and its detection limit is up to 1.39×10^{-12} mol/L.

In recent years, carbon nanomaterials have become a research hotspot in the construction and development of electrochemical sensors. In addition to increasing the specific surface of the electrode and accelerating the electron transfer rate on the electrode

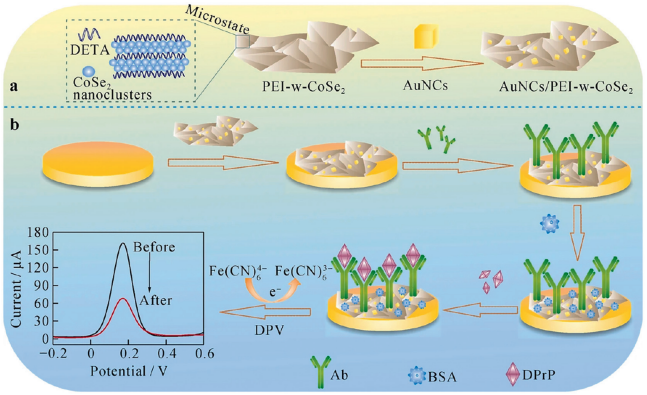

Fig. 1. Schematic diagrams for (a) constructing AuNCs/PEI-w-$CoSe_2$ and (b) electrochemical immunosensor for DPrP detection. Reproduced with permission [103]. Copyright 2021, Springer.

surface, carbon nanomaterials can also interact with target substance to be detected through the functional groups carried by themselves, so as to enrich the target material on the electrode surface and improve the detection performance of the sensor [104]. And beyond that, the important role of carbon nanomaterials in electrochemical sensing field is to serve as carrier materials to provide nucleation and growth sites for other nanomaterials with remarkable catalytic properties to prevent their aggregation during growth, thereby enhancing the catalytic performance of nanomaterials for the target substances to be detected [105]. Recently, some electrochemical sensor modified with carbon nanomaterials have been prepared for trace detection of PAEs. Due to unique chemical and electrical properties of carbon nanomaterials, the electrochemical sensors displayed enormous potential in improving selectivity, response velocity, sensitivity to satisfy the ever-increasing demand for trace detection of PAEs in various samples. Xiong *et al.* [106] synthesized a β-cyclodextrin–graphene (β-CD-G) composite using graphene and β-CD, and modified it on a glassy carbon electrode (GCE) to construct an electrochemical impedance sensor for the determination of DEHP. Based on the superb electron transfer characteristics and large specific surface area of graphene and high host-guest recognition ability of β-CD, the prepared sensor can easily adsorb massive guest DEHP molecules *via* the β-CD hosts cavities. The formed inclusion complexes (DEHP and β-CD cavity) hinder the possibility of the redox probe to approach the surface of GCE in $K_3Fe(CN)_6$ solution, an excellent linear relationship can be formed between the concentration of DEHP in β-CD–G composites and the impedance value. The electrochemical sensor represents excellent reproducibility, sensitivity and stability. The detection results showed that the impedance value increased linearly with DEHP concentration in the range of 2–18 μmol/L, the LODs was 0.12 μmol/L (3σ method), with a correlation coefficient of 0.998. To further improve the sensitivity of the sensor, Xiong and his research team [107] modified glassy carbon electrode with β-cyclodextrin/graphene/1,10-diaminodecane (β-CD-G-DAD) composite based on β-CD principle again. The impedance value increased linearly with increased DEHP concentration at the electrode modified by the composite material, in the range of 0.2 mmol/L to 1.2 μmol/L, and LODs was 0.01 μmol/L, and sensitivity of the sensor was further improved. Nonetheless, the drawback of the sensor is that the analyte only needs to form the host guest complex with β-CD. However, many phthalate ester molecules with similar structure can form the host guest complex with β-CD, which is not conducive to increasing the selectivity of the sensor. Xiao *et al.* combined the excellent electrochemical properties of ferrocene-based dendritic macromolecules with a high electron transfer efficiency of GO, prepared a novel sensitive ferrocenyl-terminated

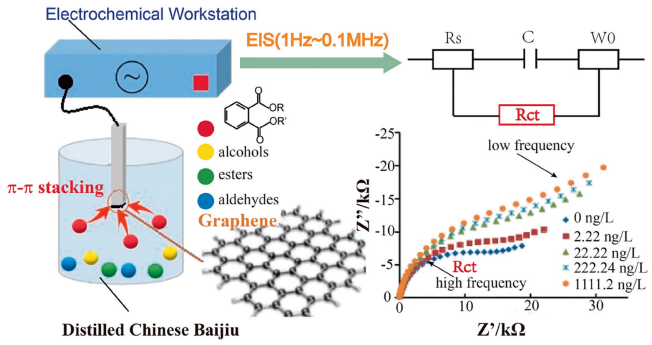

Fig. 2. A schematic diagram illustrating the basic strategies of *in situ* preconcentration and detection of PAEs in Chinese liquor with electrochemical impedance spectroscopy. Reproduced with permission [110]. Copyright 2020, the authors.

dendrimer and GO modified sensor (Fc-AED/GO/GCE) for detection of DEHP [108] and DMEP [103], respectively. Herein, graphene was used as a sensitizer due to its high surface area, dramatic electrical conductivity and feasibility for surface functionalization to enhance electrode surface area and amplify sensor signals. The combination of excellent structure and electrochemical activity of Fc-AED with excellent electron transfer of GO may remarkably boost the electron transfer between the target analyte and sensor, which is bound to help improve the sensitivity of ferrocenyl-terminated dendrimer sensors. These results showed that the modified electrode has wide linear response range, high sensitivity, outstanding selectivity and acceptable reliability to the target analyte. In contrast, the wider linear response range is more suitable for effective and timely detection of DEHP and DMEP in various consumer products. Unfortunately, the two reports did not compare the sensor's selectivity to DEHP and DMEP [108,109]. The unique structure endows graphene-based materials with large surface area and potential to establish π-π stacking interactions, owing to the delocalized electrons of graphene, which makes it an excellent adsorbent. Jiang *et al.* [110] prepared a graphene working electrode based on π-π stacking interaction between graphene and PAEs, which realized direct sampling and *in-situ* preconcentration of PAEs. Electrochemical impedance spectroscopy (EIS) was used to characterize the adsorption of PAEs on the working electrode. Fig. 2 summarizes the basic principle for phthalate sensor based on electrochemical impedance measurement utilizing graphene-modified working electrode. The purpose of this study was to establish an enrichment-free method for determination of phthalate esters in liquor *via* electrochemical impedance spectroscopy. By contrast, this is a simple, convenient, high sensitivity, very low LODs, with lower cost phthalate detection technology. However, this method lacks specificity and is not suitable for the detection of specific phthalates, and it is only suitable for the detection of total phthalates in liquor samples. Annamalai *et al.* first prepared an enzyme-based electrochemical biosensor using polyaniline, carbon nanotubes, copper nanoparticles for the detection of phthalates. The results from linear sweep voltammetric analysis indicated that the peak current gradually increased with increased DEHP concentration, and the LODs of DEHP was 0.06 nmol/L [111]. Herein, the nanocomposite materials played a role of improving electron transfer and adsorption surface area. Carbon nanotubes and copper nanoparticles maintain enzyme activity by providing a biocompatibility environment, thereby enhancing the sensitivity and catalytic electroactive surface area of the sensor. Li *et al.* [112] synthesized polyethylenimine (PEI)-functionalized N-doped graphene-$CoSe_2$ and gold nanowires (AuNWs) as a preliminary signal amplification platform for immune sensors. Thionine (Thi)-loaded Au@Pt and secondary antibody (Ab_2) connected as a signal label. The immobilized coating antigen DBP-BSA and the DBP compete for limited antibody binding sites. The concentration of DBP can be determined by DPV and SWV mode with detection limits of 0.486 pg/mL (DPV) and 0.711 pg/mL (SWV), respectively. The sensor prepared by the composite material exhibited excellent selectivity, reproducibility and stability, and can be used for sensitive detection of DBP in actual samples.

In general, the application of nanomaterials presents a tremendous potential for amplification of electrochemical signals. Up to now, the NMs used to detect PAEs comprising metal nanomaterials, nano-metal oxides, other carbon nanomaterials from NMs, are currently used for EC detection of PAEs, as shown in Table 1.

2.1.2. Electrochemical sensors based on MIP for PAEs detection

From the above, we know that the EC sensors can be applied to detect trace PAEs in complex substrates, nevertheless, there still exist some defects, such as non-specific binding, lower mass transmission, poor regeneration and limited response for EC sensor application. Therefore, highly selective sensing materials have been developed to overcome these problems. Molecularly imprinted polymers (MIP) are one of the ideal sensing materials [113,114]. The molecular imprinting technology has been established as an effective strategy for selective recognition of relevant analyte molecules in the presence of other potential interferences [115–118]. The principle is that the template molecule and functional monomer are synthesized into host-guest complex, and then quantitative functional monomer and cross-linking agent are added to polymerize the polymer. The template molecules are thereafter embedded in a polymer of functional monomer [119]. After the template molecules are extracted and eluted, imprinted cavities are left in the polymer. MIP can selectively recognize and bind specific analytes through noncovalent strength interactions between the host matrix and guest molecule [120–123], based on shape, size, and functionalities of the imprinted cavities specifically complementary to the template molecules. The imprinted polymers have the characteristics such as high selectivity, physiochemical stability, robustness, longer shelf life, reusability and specific recognition of analyte and structurally related compounds [124,125]. By organically combining molecularly imprinted technology with sensor detection technology, we can take full advantage of the high selectivity of MIP and high sensitivity of sensor detection signal to prepare molecularly imprinted sensors with anti-interference, high selection and high sensitivity [126,127]. In 1987, Tabushii *et al.* [128] prepared an electrochemical sensor using molecularly imprinted polymer as a sensitive material for the first time and successfully detected vitamins. Ever since, the molecularly imprinted electrochemical sensor has aroused wide interest and become a research hotspot [125,129-130].

Zia *et al.* [124] synthesized a selective MIP for DEHP by suspension polymerization, and it was applied to a novel interdigital capacitive sensor for real-time non-invasive detection of phthalates in water-mixed samples using electrochemical impedance spectroscopy (EIS). Frequency response analyzer (FRA) algorithm was applied to achieve impedance spectra, thus determining sample conductance and capacitance for evaluation of phthalate concentration in the sample solution. The influence of surface immobilized molecular imprinted polymer layer on circuit parameters and its electrical response was deduced by principal component analysis (PCA). The results obtained by the test system were verified by high performance liquid chromatography-diode array detector. Zhao *et al.* [131] reported a novel EC sensor for diisononyl phthalate (DINP) analysis. The electrode of the sensor was modified by the mixture between DINP MIPs and agarose in proportion. The MIPs were synthesized by bulk polymerization *via* non-covalent multiple interactions. Cyclic voltammetry (CV) was used to establish an analytical method for DINP by molec-

Table 1
Nanomaterials used for electrochemical detection of PAEs.

NMs	EC platform	EC technique	Analyte	Sample matrix	Linear range	Detection limit	Recovery (%)	Ref.
Pt	AuPt–GS/GCE	DPV	DMP	Water	5.1 nmol/L-5.1 μmol/L	1.69 nmol/L	92–108	[100]
Au	Au/SiO_2	EIS	DEHP	Water	5.13 nmol/L-5.13 μmol/L	[b]	[c]	[101]
Au, MWCNTs, GONRs	Chitosan/MWCNTs@GONRs/GCE	EIS	DBP	Environmental water	[a]	25 nmol/L	86.0–120.4	[102]
$CoSe_2$, AuNC	AuNCs/PEI-w-$CoSe_2$	CV/DPV/EIS	DPrP	Liquor	10 pmol/L-10 μmol/L	1.39 pmol/L	95.18–101.1	[103]
Graphene	β-Cyclodextrin–graphene/GCE	EIS	DEHP	Wastewater samples	2–18 μmol/L	0.12 μmol/L	99.1–101.4	[106]
Graphene	β-Cyclodextrin/graphene/1,10-diaminodecane/GCE	EIS	DEHP	Wastewater samples	0.2–1.2 μmol/L	0.01 μmol/L	98.3–101.2	[107]
Graphene oxide	Fc-AED/GO/GCE	DPV	DEHP	Daily alcohol aqueous	0.6–1000 μmol/L	0.9 μmol/L	[c]	[108]
Graphene oxide	Fc-PED/GO/GCE electrochemical sensor	DPV	DMEP	Daily alcohol aqueous	0.06–1200 μmol/L	0.04 μmol/L	[c]	[109]
Graphene	G/GCE	EIS	DEP	Chinese liquor	0.1–5 nmol/L	0.108 pmol/L	[c]	[110]
MWCNTs	EST/PANI/CNTs/CuNPs-NF/GCE	LSV	DEHP	PET bottle stored drinks and lake water	[a]	0.06 nmol/L	[c]	[111]
N-doped graphene/$CoSe_2$ nanobelt	AuE/PEI-NG-$CoSe_2$/AuNWs/DBP-BSA/BSA/Ab_1/Thi-Au@Pt-Ab_2/GCE	DPV SWV	DBP	Liquor	3.59 pmol/L-3.59 μmol/L	1.74 pmol/L 2.55 pmol/L	101.75–107.13 100.47–106.25	[112]

[a] No linear range.
[b] No detection limit.
[c] No recovery.

ularly imprinted sensors. The experimental results showed that the prepared imprinted membrane had high selectivity and distinct sensitivity for DINP, with linear range of 50–1000 nmol/L and detection limit (LODs) of 27 nmol/L. The novel sensor provides brand-new possibilities for real-time detection without pretreatment of sample. The recovery rate for real sample analysis in liquor samples was 105.3%−115.7%, and the relative standard deviation (RSD) was 0.4%−1.2%. Molecularly imprinted polymers (MIPs) were combined with magnetic nanomaterials to prepare magnetic molecularly imprinted nano-sensitive films. To a certain extent, this method can not only overcome the defects of molecularly imprinted polymers, such as uneven distribution of molecularly imprinted sites, low binding amount, partial mosaic of binding sites, but also significantly improve the sensitivity and selectivity of sensors. Zhang *et al.* [132] developed a highly sensitive and selective MIP sensor combined with magnetic molecularly imprinted solid phase extraction (MMI-SPE) for the determination of DBP in complex matrixes. Under the optimized experimental conditions, the response currents of the MIP-sensor exhibited a linear relationship towards DBP concentrations ranging from 1.0×10^{-8} g/L to 1.0×10^{-3} g/L. The limit of detection of the MMIP-sensor coupled with the MMISPE was calculated as 0.052 ng/L. Using gold-modified magnetic graphene (Au@Fe_3O_4@RGO) as a carrier, Li *et al.* [133] prepared gold-modified magnetic graphene-based molecularly imprinted composites (Au@Fe_3O_4@RGO-MIP) by surface molecular imprinting technology. A molecularly imprinted electrochemical sensor was constructed using Au@Fe_3O_4@RGO-MIP modified glassy carbon electrode. The sensor displayed good responsiveness and selectivity to plasticizer DBP, which provided a new method for DBP detection in water environment. The results show that the equilibrium time of the sensor for DBP in water environment is 6 min. In the concentration range of 0.01–0.1 μmol/L, there is a good linear relationship between DBP concentration and response current. The minimum detection limit is 0.3049 nmol/L (S/N = 3). Electro polymerization is a simple and effective technique to construct molecularly imprinted polymer electrochemical sensors. Gulcin Bolat *et al.* [49] synthesized molecularly imprinted conductive compound polypyrrole (PPY) by electrochemical polymerization of pyrrole. Electrosynthetic PPY is one of the most widely applicable polymers in the development of imprinted films, and it has sensitive electrochemical impedance sensing performance, and can also be applied for trace detection of DBP. The team characterized the DBP imprinted polypyrrole sensor *via* cyclic voltammetry, and their results showed that the sensor was distinctly sensitive. The detection limit obtained by electrochemical impedance spectroscopy (EIS) was as low as 4.5 nmol/L, and the linear response was in the concentration range of 0.01–1.0 μmol/L. Zhou *et al.* [134] developed a highly selective and highly sensitive dibutyl phthalate electrochemical sensor (MIP-DBP-CTS/F-CC_3/GCE) by electrodeposition of DBP-CTS polymer on F-CC_3 (a functional corncob biochar)-modified GCE. The detection results of cyclic voltammetry (CV) and electrochemical impedance spectroscopy (EIS) show that the F-CC_3 layer and the DBP-CTS molecularly imprinted polymers of the MIP-DBP-CTS/F-CC_3/GCE have synergistic fast electron transfer capability, and large electrochemical area, which can help to amplify the electrochemical signal and thus enhance the sensitivity of the sensor, as shown in Fig. 3.

Although molecular imprinting technology (MIT) has significant advantages and diverse applications, it faces a number of challenges, such as imprinting sites are inside the polymer, template molecules are not easy to elute, which will lead to incomplete template removal, fewer binding sites and slow mass transfer, *etc.* [126,135]. In addition, the MIPs are usually synthesized using target analytes as templates. Therefore, there is a possibility of template leakage, which may influence the consequence of quantitative analysis [136]. This also restricts the applications of

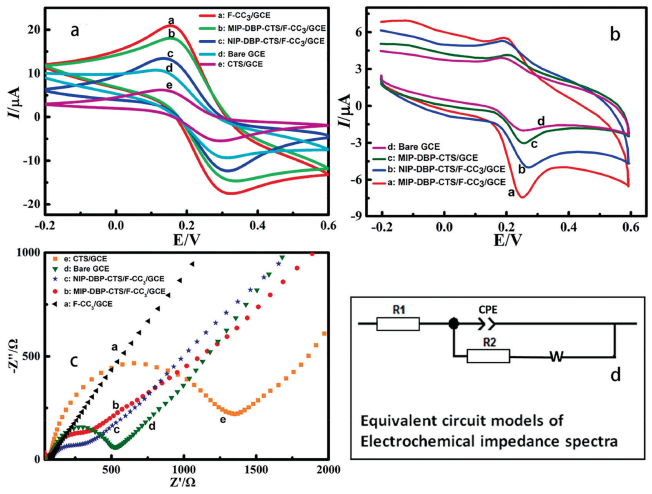

Fig. 3. (a) Cyclic voltammetric responses of different electrodes at the range of −0.2–0.6 V at 100 mV/s in 5 mmol/L $K_3[Fe(CN)_6]$. (b) CVs of different electrodes in 0.01 mol/L PBS (pH 7.0) containing 5 mmol/L $K_3[Fe(CN)_6]$ after adsorption in 1.8 μmol/L DBP for 120 s. (c) The electrochemical impedance spectrum (EIS) was recorded in 5 mmol/L $K_3[Fe(CN)_6]$. (d) Equivalent circuit models of electrochemical impedance spectra (R_1: a constant solution resistance, R_2: charge transfer resistance (R_{ct}), W: Warburg impedance, CPE: characterization of electrical double-layer capacitor constant phase element). Reproduced with permission [134]. Copyright 2021, Elsevier.

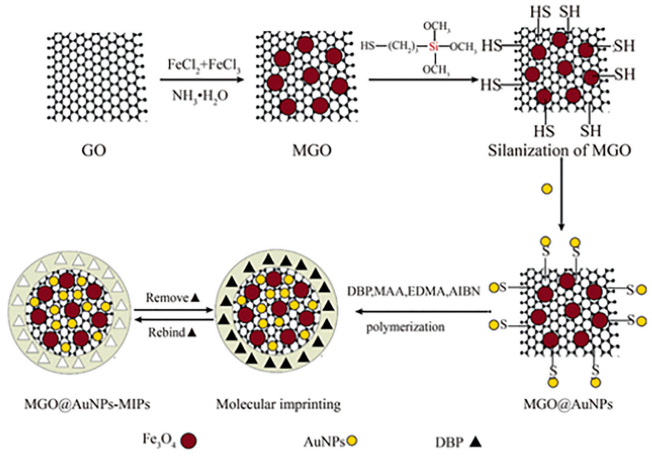

Fig. 4. Illustrations of fabrication procedure for MGO@AuNPs-MIPs. Reproduced with permission [140]. Copyright 2014, Elsevier.

MIT in various aspects. Therefore, on this basis, surface molecular imprinting technology (SMIT) was gradually developed. Surface molecular imprinting refers to the technique for imprinting the surface of the solid phase matrix by polymerization reaction, so that the molecularly imprinted recognition sites are distributed on the surface of the molecular imprinted polymer or on the outer layer of the solid phase matrix and on surface [137,138]. This molecularly imprinted material has significant benefits different from other methods, for instance, the binding site is easily obtained, the material migration and binding kinetics are accelerated, the separation efficiency of imprinted materials is improved, and biological macromolecules such as proteins can be imprinted [139]. In addition, it can also decrease non-specific adsorption and "embedding" phenomenon. Li *et al.* [140] successfully synthesized a molecularly imprinted membrane that selectively recognized DBP on MGO@AuNPs composite substrate (Fig. 4). Due to the unique mechanical properties and large surface area of MGO (magnetic graphene oxide) nanoparticles, more binding sites are provided for template recognition, and the majority of the binding sites widely distributed on or approach to the surface of the externally imprinted polymer layer. The prepared MGO nanoparticles/molecularly imprinted polymer composites therefore own prominent selectivity compared with other analogs and remarkable sensitivity to template molecules. The electrode modified by MGO@AuNPs-MIPs can recognize DBP specifically. Under optimal experimental conditions, the linear concentration range of DBP selectively detected is $2.5 \times 10^{-9} \sim 5.0 \times 10^{-6}$ mol/L, and the new DBP electrochemical sensor also shows excellent repeatability. Li and Zhong *et al.* [120] described a molecularly imprinted polymer photoelectrochemical sensor based on bismuth sulfide (Bi_2S_3) for determination of DOP. MIP membranes that can specifically recognize DOP molecules were electropolymerized onto Bi_2S_3/ITO surfaces *via* cyclic voltammetry. With Bi_2S_3 as photoelectric converter for the sensor, visible light as the excitation source, and generated photocurrent as the detection signal, the relationship between photocurrent and concentration of the analyte was quantitatively detected. Under optimum experimental conditions, the photoelectrochemical response is proportional to logarithm of DOP concentration in the range of 0.5–70 pmol/L, with a detection limit of 0.1 pmol/L. Compared with previous methods, the sensitivity of this method has achieved significant improvement. This method has superiorities of short detection time and low preparation cost, and provides a new effective method for DOP detection. Unfortunately, due to logarithmic response to concentration of analyte, it still has the limitation of low system resolution. Latest research also depicts that molecular imprinting technique has rigorously been used for the electrochemical detection of trace phthalate analytes in complex matrix, as shown in Table 2.

Photoelectrochemical (PEC) sensor is an emerging technology as the advantage of fast response, high sensitivity and uncomplicated operation [141]. The simple and novel PEC sensors have been developed for the detection of various chemicals. Based on MIP modified $Cu_3(BTC)_2$@Cu_2O heterostructure, Gao *et al.* [142] designed a novel dioctyl phthalate (DOP) PEC sensor, which was constructed by imprinting DOP on the heterostructure using $Cu_3(BTC)_2$@Cu_2O heterostructure as the photoelectric converter. The PEC sensor for detection DOP showed a low detection limit of 9.15 pmol/L.

2.1.3. Electrochemical sensors based on aptamers for PAEs detection

Electrochemical aptasensors consist of electrodes and electrochemically active recognition molecules. After the aptamer fixed on the electrode surface is combined with the target, the target concentration is detected by collecting the variation of electrochemical signals, such as voltage, current, conductivity and impedance [143–145]. Nucleic acid aptamer is a new type of biological recognition element [146–149]. It was applied in electrochemical sensors for the first time since 2004 [150]. Due to its advantages such as strong specificity, good stability, *in vitro* synthesis and small molecular weight, it has rapidly attracted the attention of many scholars [151–154]. Electrochemical sensors based on nucleic acid aptamers have greatly promoted the development of electrochemical sensing technology due to their fast detection speed, simple and easy operation of the equipment, wide detection range, noble specificity and significant sensitivity, and have been widely used in environmental monitoring [155], food safety [156], medical detection [157] and clinical diagnosis [158] and other fields. However, electrochemical aptamer sensors for highly hydrophobic small molecular targets (such as phthalates) are rarely reported. Compared with proteins and other macromolecules, PAEs molecules are small, and they have extremely poor water solubility and lack functional groups for surface immobilization. The screening of PAEs aptamers is therefore challenging. Han *et al.* [159] successfully screened group-specific phthalate aptamers *in vitro* through reasonably designed target fixation strategies. And for the first time, they achieved the identification of group-specific PAE-binding DNA

Table 2
MIP used for electrochemical detection of phthalate esters.

PAEs	Detection method	MIP film composition	Linear range	Detection limit (LODs)	Samples	Recovery (%)	Ref.
DEHP	EIS	*N*,*N*-Methylene-bisacrylamide, dimethlyformamide, tetramethylethylenediamine (TEMED), ammonium persulfate	64-130 nmol/L	-[a]	Artificial saliva	≥90	[130]
DEHP	EIS	Meth acrylamide, *N*,*N*-methylene-bisacrylamide, ammonium persulfate	2.56–256 μmol/L	-[a]	Water	-[c]	[124]
DINP	CV	*α*-Methyl acrylic acid, ethylene glycol dimethacrylate, acetonitrile, azodiisobutyronitrile	50–1000 nmol/L	27 nmol/L	Distilled liquor	105.3–115.7	[131]
DBP	CV/DPV	Methacrylic acid, ethyleneglycol dimethacrylate, azodiisobutyronitrile	36 pmol/L-3.6 μmol/L	18.6 pmol/L	Soybean milk, milk	96.10–100.6	[132]
DBP	CV/DPV/EIS	Methacrylic acid, azodiisobutyronitrile, divinyl benzene	0.01–0.1 μmol/L	0.3049 nmol/L	Water	-[c]	[133]
DBP	EIS	Polypyrrole	0.01–1.0 μmol/L	4.5 nmol/L	–[b]	-[c]	[49]
DBP	CV/DPV/EIS	Chitosan, glutaraldehyde	0–1.8 μmol/L	0.0026 μmol/L	Rice wine	90–92	[134]
DBP	DPV	Methacrylic acid, ethylene glycol dimethacrylate	2.5 nmol/L-5.0 μmol/L	0.8 nmol/L	A brand wine drinks	97–104	[139]
DOP	DPV/EIS	*o*-Phenylenediamine (*o*-PD)	0.5–70 pmol/L	0.1 pmol/L	Plastic bottled water, wastewater, and soil extracts	96.17 and 104.2	[120]

[a]No detection limit.
[b]No samples.
[c]No recovery.

aptamers *via* integration of proper design of initial targets with high-throughput sequencing technology. The PAE-aptamers possess the highly conserved cytosine-rich sequences and show good group selectivity to PAEs that contain both the ester and the benzoyl groups. The constructed PAEs aptamer sensor can detect DEHP at a detection limit of 10 pmol/L (3S/N) and dynamic range of 10 pmol/L to 100 nmol/L. A linear relationship can be observed between signal reduction and logarithm of DEHP concentration. Subsequently, Han and their team immobilized synthesized amino functionalized dibutyl phthalate (DBP-NH_2) as an anchor target on the epoxy-activated agarose beads according to a bead-based method, so that the phthalate groups were displayed on the surface of the immobilization matrix, aiming at selecting group-specific aptamers for phthalates (Fig. 5). Based on the obtained aptamer, a highly sensitive electrochemical sensor for specific detection of DEHP was fabricated [160]. Lu *et al.* [161] selected aptamers specific for DEHP from an immobilized ssDNA library applying the systematic evolution of ligands by exponential enrichment (SELEX) and established an EIS aptasensor for direct detecting DEHP residue in water samples with a LODs of 0.103 pg/mL.

Combination of the recognition aptamer and PEC techniques, Shen *et al.* [162] designed a label-free PEC aptasensor based on perovskite for detection of dibutyl phthalate (DBP). Herein, cetyltrimethylammonium bromide (CTAB) was chosen to improve the stability and performance of $CH_3NH_3PbI_3$ perovskite, which has a strong electrostatic interaction with the aptamer and promote the assembly of the aptamer on the $CH_3NH_3PbI_3$ surface. The aptamer impedes the transfer of the photogenerated electrons from perovskite to the electron acceptor in solution due to the block effect. When DBP is present in solution, the binding affinity between DBP and the aptamer competes with electrostatic interaction between aptamer and CTAB, resulting in dissociation of the aptamer from the electrode and the recovery of the photocurrent. The displacement of the aptamer from the perovskite surface enhances the photoelectric signal of perovskite. The linear range

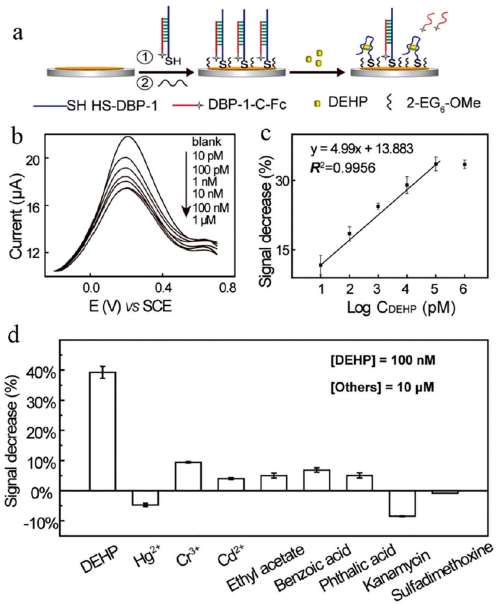

Fig. 5. PAE SD-EAB for ultrasensitive and ultraselective detection of DEHP: mechanism (a), SWV curves (b), calibration curve (c), and selectivity tests (d). Reproduced with permission [159]. Copyright 2017, American Chemical Society.

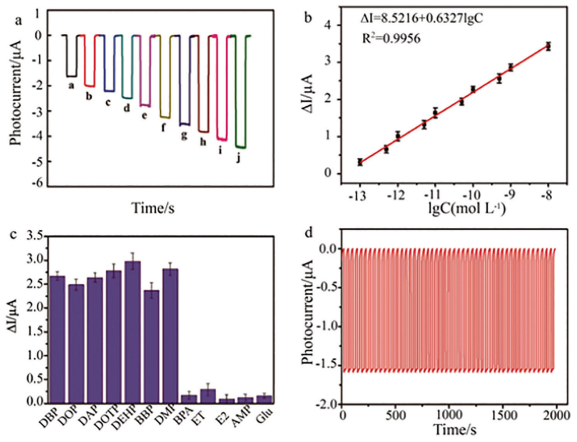

Fig. 6. (a) Photocurrent responses of the PEC aptasensor incubated with different concentrations of DBP (from a to j: 0.1 pmol/L-10.0 nmol/L). (b) Calibration curve of photocurrent response changes of the PEC aptasensor (ΔI) to different concentrations of DBP. (c) Selectivity of the PEC aptasensor incubated with 1.0 nmol/L different PAEs and 10.0 nmol/L different interferences. (d) Stability of the PEC aptasensor under continuous detection. Error bars were derived from the standard deviations of three measurements. Reproduced with permission [162]. Copyright 2022, American Chemical Society.

of the PEC sensor for detection DBP was from 1.0×10^{-13} mol/L to 1.0×10^{-8} mol/L with the detection and quantification limits 2.5×10^{-14} and 8.2×10^{-14} mol/L (S/N = 3), respectively, shown as Fig. 6.

2.2. Optical sensors for determination of phthalate esters

Compared with electrochemical sensors, optical sensors have less interference with the detection system, which is commonly used to detect target substances. The optical sensor is a detector that measures the optical properties of materials and converts their optical signals into other signals (such as the conversion of optical signals to electrical signals). The optical sensors can produce changes in optical signals in the combination process, so as to detect the content of target analyte according to changes of optical signals [163]. According to different optical signals, the optical technology can be divided into the following types: Fourier-transform infrared spectroscopy (FTIR), UV–visible spectrum [164], fluorescence [165–168], Raman scattering, chemiluminescence [169] and so on [170,171]. And among them, FTIR can detect PAEs rapidly, but has low sensitivity and cannot detect low concentrations. Moreover, their detection limits are usually considerably higher than the regulatory criteria [172]. Here, progress of the optical sensors for the detection of phthalates are introduced ultraviolet-visible spectroscopy sensors, fluorescence spectroscopy sensors, surface enhanced Raman scattering sensors and chemiluminescence sensors.

2.2.1. Ultra violet-visible spectroscopy sensors for determination of phthalate esters

Compared with other sensors, colorimetric sensor is based on analysis of color change, which directly or indirectly realizes the qualitative and quantitative detection of the target object causing color change through naked eye observation or spectrophotometer. It has the characteristics such as visible, readable, easy to operate, low cost, fast detection speed, real-time, on-site analysis, no need for any expensive, precise or complex instrument. It has been widely applied to environmental pollution monitoring [173], drug residues analysis [174], disease diagnosis [175], food safety monitoring [176], and biochemical analysis [177]. The introduction of nanomaterials, metal-organic framework materials (MOFs) [178] and aptamers [179,180] has promoted the rapid development of colorimetric sensors, which has become one of important analytical methods for rapid and simple determination of various targets. Based on characteristics of Au NPs that can adsorb single-chain nucleic acid aptamers, and they are easy to aggregate and discolor, Guo and his research team [181] constructed a colorimetric sensor based on Au NPs, which quickly and simply realized the detection of DEP, DBP and DEHP. Since the aptamer has extreme flexibility and can be strongly linked to AuNPs through covalent bonds between AuNPs and thiol groups on DNA to form DNA-modified AuNPs, an anti-aggregate and the color of the sample is red at that very moment. With addition of phthalates in the test sample, specific recognition between aptamer and PAEs occurs and the color changes from red to blue with increased concentration of PAEs. The results showed that DNA modified AuNPs had good sensitivity and selectivity for the detection of phthalates. The detection limits for DEHP, DBP and DEP were 0.144 ppm, 0.077 ppm, and 0.026 ppm, respectively. Yan *et al.* [182] used L-arginine functionalized gold nanoparticles (ARG-AuNPs) as sensing probes for DBP detection to prepare a colorimetric sensor with high selectivity and sensitivity. The presence of carboxyl, amino and guanidine groups in L-arginine leads to a high affinity between ARG-AuNPs and DBP, which contributes to the aggregation of ARG-AuNPs and the solution color changes from red to blue. The color change of solution can be used to semi-quantify DBP content. In addition, this method has good selectivity and does not need sample preparation technology and complicated operation to detect DBP in liquor rapidly and semi-quantitatively. MOFs materials are often used for the analysis of targets due to their excellent properties, such as large surface area, ordered pore structure, multiple coordination positions and high loading capacity [183]. Zhu *et al.* [184] prepared a sensitive colorimetric immunosensor for rapid detection of trace DBP using Cu-MOFs and horseradish peroxidase (HRP). Cu-MOFs were labeled on the second antibody (Cu-MOFs@Ab_2) for signal amplification. When MOFs@Ab_2 is captured by antigen-antibody (Ab_1) complexes, large amounts of copper(II) will be released from Cu-MOFs in the presence of nitric acid (HNO_3). The addition of sodium ascorbate (SA) further reduced copper(II) to copper(I) and inhibited the HRP to catalyze the colorless 3,3′,5,5′-tetramethylbenzidine (TMB) into blue oxidized TMB (ox TMB). The detection limit for the sensor is nearly 60 times lower than that of conventional ELISA with the same antibody. Recently, key characteristics of localized surface plasma resonance (LSPR) of noble metal NP sensors based on colorimetric approach, the induction of target analyte will lead to aggregation or dispersion of chemically functionalized nanoparticles and reversible color change of the solution [185]. Moreover, Cu^{2+} can form hybrid metal–phthalate scaffolds with phthalate and their derivatives. Based on these principle, Zhang *et al.* [186] constructed a colorimetric sensor utilizing uridine-5′-triphosphate (UTP)-modified gold nanoparticles (U-AuNPs) as color indicator and Cu^{2+} as across-linker. The aggregation of U-AuNPs was induced by phthalates in the presence of Cu^{2+}, with the color changing of U-AuNPs from red to purple. The sensor demonstrated superior sensitivity at a detection limit of phthalates of 0.5 ppm. Furthermore, based on the characteristics of M-13 phage layer, such as fast response to external stimuli and reliable discoloration behavior, Seol *et al.* [187] also investigated M-13 phage color sensor with the potential to analyze four phthalate esters (bis-(2-ethylhexyl)-phthalate (BEHP), dibutyl phthalate (DBP), diethyl phthalate (DEP) and benzyl butyl phthalate (BBP) with similar molecular structure. Kang *et al.* [188] prepared molecular surface imprinted graft copolymer MIPs@MOF-5 by free radical polymerization. The imprinted site was fixed on the surface of MOF through the surface molecular imprinting process, thus improving the adsorption capacity, recognition ability and separation efficiency of dibutyl phthalate. The molecularly imprinted polymer

MIPs@MOF-5 has high sensitivity and selectivity by combining the advantages of molecularly imprinted polymer and metal-organic framework, which was analysized sensitively and selectively the dibutyl phthalate of tap water sample.

2.2.2. Fluorescence sensors for determination of phthalate esters

As an emerging means of analysis and testing, fluorescent sensors have attracted wide attention of researchers due to their, convenience, prominent selectivity, real-time online detection, short response time, remarkable sensitivity and accuracy [189,190]. In recent years, great progress has been achieved in the research and application of fluorescent sensors [191,192]. In particular, the fluorescence analysis technology of rare earth luminescent complexes and luminescent quantum dots can eliminate the interference of various scattering light generated by short-life instruments and background fluorescence from samples and reagents on the detection, which greatly improves the accuracy of fluorescence chemical determination [193]. Wei *et al*. [194] prepared luminescence sensors based on lanthanide organic frameworks, $[Ln(tftpa)_{1.5}(2,2'\text{-bpy})(H_2O)]$ (Ln = Gd 1, Eu 2 and Tb 3, H_2tftpa = tetrafluoro terephthalic acid), for the detection of dibutyl phthalate in simulated seawater with detection limit of 2.07 ppb. As fluorescent probes, Ln-MOFs can be reused multiple times in addition to simple, fast response time and high sensitivity, which provides an opportunity for the exploration of reversible and recyclable luminescent sensors. In particular, luminescent quantum dots (QDs) have attracted much attention due to their outstanding optical properties, such as high fluorescence efficiency, narrow symmetric emission, wide absorption and light stability [195]. Li *et al*. [196] prepared molecularly imprinted polymers with Mn-doped ZnS quantum dots (ZnS:Mn QDs) using it as a direct, rapid, simple and selective detection system for selective recognition of DBP in real samples. The combination of a surface-imprinted polymer and fluorescence property of QDs can improve selectivity and sensibility of fluorescence sensors. The sensor can detect DBP in the concentration range of 5.0–50 μmol/L with a detection limit of 0.27 μmol/L. Based on CdTe quantum dots and imidazoline molecular sieve framework-67, Chen *et al*. [197] developed a novel near infrared fluorescence molecularly imprinted sensor by sol-gel polymerization, which was used for rapid and sensitive determination of DBP in food (only 1.5 min). The fluorescence imprinted sensor provides a rapid detection method for DBP with a linear response concentration range of 0.05–18.0 μmol/L and a detection limit of 1.6 nmol/L. Compared with traditional CdTe QDs, ZnS QDs and ZnSe QDs are more attractive because they exhibit less toxicity and environmental problems. In their subsequent research, their team also synthesized ZnS:Mn QDs and magnetic Fe_3O_4 molecularly imprinted polymers for DBP detection. The polymers combined the merits of specific molecular recognition properties of MIPs, magnetic separation, and fluorescence characteristics of Mn–ZnS. The detection limit of the prepared fluorescence sensor was further reduced than that mentioned above, reaching 0.08 μmol/L [198]. In order to overcome the possible shortcomings of molecularly imprinted polymers, such as incomplete removal of template molecules, slow mass transfer rate, weak embedding depth and binding force, Wang *et al*. [199] used a novel and simple imprinting technique, which is surface molecular imprinting technique, using it for polymer layer synthesis on the surface of supporting nanomaterial. They synthesized a surface molecularly imprinted polymer fluorescent sensor for the detection of DEHP based on ZnO QDs with a LODs of 1.3 nmol/L. Based on Mn-doped ZnS quantum dots, Zhou *et al*. [200] fixed the imprinting site on the surface of silica nanoparticles through the surface molecular imprinting process, and prepared a new type of fluorescent molecularly imprinted polymer (SiO_2@QDs@MIPS), which integrated the advantages of excellent fluorescence performance of quantum dots and high selectivity of surface molecularly imprinted polymers. And the products can recognize sensitively and selectively dibutyl phthalate (DBP) in the range of 5–50 μmol/L, with a correlation coefficient of 0.9974. The combination of the aptamer and quantum dots further improved the sensitivity, intuition and specificity of the sensor. Wang *et al*. [201] reported for the first time a sensitive and specific fluorescent ratio immunosensor method for detection of dibutyl phthalate by combining dual-emission carbon quantum dots (CDs) with nucleic acid aptamers. Compared with single-wavelength emission method, this method can effectively overcome the instability caused by probe concentration change, instrument background interference and external interference, and the accuracy of the results was higher, which can be used for high sensitivity detection of DBP in food samples. Under the optimum conditions, the linearity range for the DBP detection method was 12.5–1500 μg/L and detection limit was 5.0 μg/L. Wang and their team [202] proposed a dual emission ratio fluorescence sensor system based on aptamer recognition of molybdenum disulfide quantum dots (MoS_2 QDs) and cadmium telluride quantum dots (CdTe QDs) to detect DEHP in pork. Amidation between aptamers and CdTe QDs were close to the distance between CdTe QDs and DEHP, resulting in fluorescence quenching of CdTe QDs. MoS_2 QDs transmit self-calibration signal, its fluorescence remains almost constant when co-existing with DEHP. The LODs for the prepared dual emission ratio fluorescence sensor was 0.21 μg/L, which was successfully applied in the determination of DEHP in pork. Lim *et al*. [203] developed a QD-aptasensor for the detection of DEHP and its accompanying portable analyzer. The QD-aptasensor showed excellent DEHP selectivity and sensitivity with a limit of quantitation (LOQ) = 0.5 pg/mL. The equivalence between the developed portable analyzer based on QD APtasensor and the laboratory protocol was also established. The DEHP concentration ranges from 0.0005 ng/mL to 100 ng/mL, and the correlation coefficient $r = 0.86$. In addition, Dolai *et al*. [204] reported the fluorescence selective detection of dibutyl phthalate (DBP) based on the poly-cyclodextrin-graphene oxide (GO) nanocomposite. The molecular imprint inside the nanocomposite can selectively capture DBP, and GO offers fluorescent "turn on" DBP detection. The nanocomposite-modified paper strip showed a linear calibration range of 0.025–1 mmol/L in the DBP concentration with a LOD of 0.024 mmol/L.

The restriction of dynamic intramolecular motions in the solid state decreases the nonradiative process and thereby increases the emission efficiency. Based on the phenoment, Qiu *et al*. [205] fabricate porous crystalline ribbons that enable noncovalent binding of phthalate molecules from a trifluorene molecule end-substituted by nitrophenyl groups. Phthalate molecules can suppress the rotation of nitrophenyl groups in the caves of ribbons *via* noncovalent interactions, thereby enhanced emission. On the basis of this novel response mechanism, fluorescence detection of phthalates with high sensitivity (the limit of detection DEHP is 0.03 ppb) (Fig. 7). In addition, supramolecular host enble to bind hydrophobic small molecules fluorophore in its interior. Based on the phenomenon, Cromwell *et al*. [206] report a new method using cyclodextrin-promoted fluorescence detection. In the presence of the phthalate analytes, the fluorescence emission signal of a fluorophore 17 bound in a cyclodextrin cavity leads to highly analyte-specific changes. The large cavity of cyclodextrin facilitates association between the phthalate analytes and the fluorophore, further restricting the free rotation of the fluorophore and increasing the observed fluorescence emission. Using this method, 15 phthalate esters were detected with highly analyte-specific responses.

2.2.3. SERS sensors for determination of phthalate esters

SERS (surface enhanced Raman scattering) technology is a new spectroscopic technology which adsorbs the target on the sur-

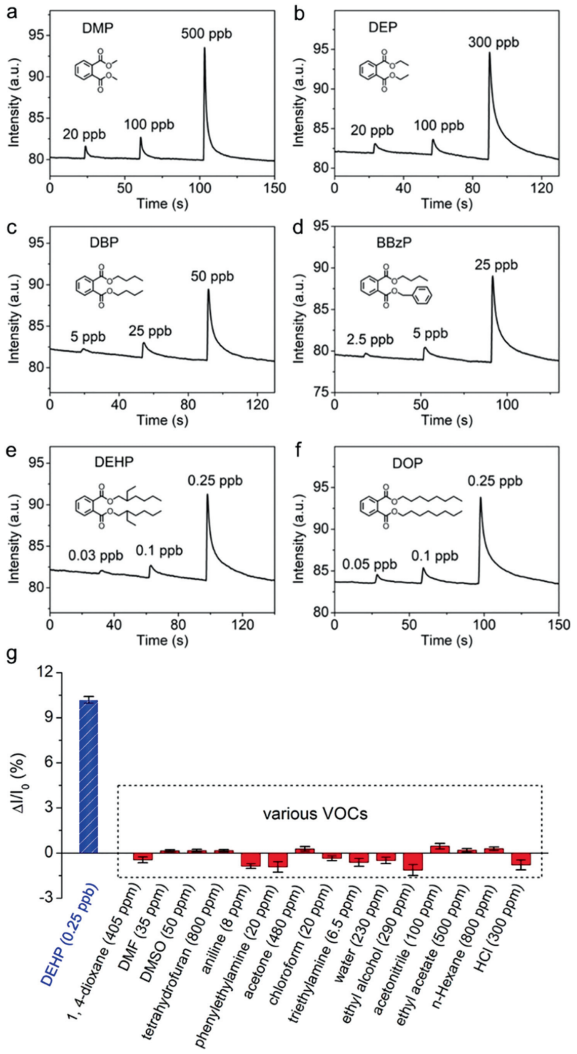

Fig. 7. (a-f) Time-course curves of fluorescence responses of flower-like 1 microsheets upon exposure to phthalate vapors at different concentrations. (g) Columnar comparison of fluorescence responses of flower-like 1 microsheets upon exposure to DEHP and other different interfering agents at various concentrations. $\Delta I/I_0$ represents the change of fluorescence intensity. Error bars represent the standard deviation of five measurements. Reproduced with permission [205]. Copyright 2019, American Chemical Society.

face of nanomaterial and enhances the signal during Raman spectroscopy test, even up to 15 orders of magnitude. Owing to their characteristics, such as simple processing process, convenient and quick detection, less damage to samples, and providing molecular fingerprint, SERS is extremely suitable for rapid detection on site. Over the years, it has been widely used in the analysis and identification of trace substances, covering forensic identification, food safety, biomedical science, trace drugs, environmental pollution and other aspects [207,208]. The relationship between intensity of Raman characteristic peaks and concentration of PAES can be studied by the enhancement of Raman spectra of PAEs with Raman-enhanced active substrate. Raman spectroscopy is analyzed to establish a mathematical model, so as to achieve quantitative analysis of a variety of PAES, which will point out a new direction for trace PAES detection. The magnitude of Raman signal enhancement is related to the shape, structure, surface characteristics and aggregation state of nano-molecules for the materials with surface-enhanced Raman effect. The development of new SERS enhanced substrate is therefore one of the core issues in the SERS technology. The reported Raman-enhanced active materials for PAES trace detection mainly include gold nanoparticles, silver nanoparticles, and some semiconductor–noble-metal nanocomposites. Wang *et al.* [209] prepared large-area dense nanomembranes by self-assembly at liquid-liquid interface with the synthesized gold nanotriangles, and then transferred the nanomembranes to the surface of filter paper by capillary effect to make SERS substrate membranes. The results showed that the concentration of BBP in liquor could be detected as low as 1×10^{-8} mol/L. This kind of SERS substrate membrane showed a fast detection speed, high sensitivity, convenient operation, and a great potential for SERS analysis. Zuo *et al.* [210] used Ag nanoparticles (NPs) decorated Si nanocone (SINC) array as an effective SERS substrate for high sensitivity detection of PAEs, and this substrate has high enhancement and excellent uniformity for the detection of trace dimethyl phthalate (DMP) at a concentration of 10^{-7} mol/L. Wu *et al.* [211] prepared uniform gold nanoparticles membrane by utilizing the solvent-driven self-assembly strategy, using it as an active SERS substrate to realize the sensitive detection of DEHP in different wines and sweet drinks at 0.1 ppm level. However, a single metal as the active substrate has certain limitations, since the oxidation of Ag nanostructure leads to rapid degradation of SERS activity, and the SERS signal provided by Au nanostructure is inferior to that of Ag. Bimetallic composite system can play a synergistic effect, which integrates the absorption bands from two metals, and has better Raman scattering enhancement effect. Cao *et al.* [212] first synthesized two different microstructures, the Ag_2S particles inlaid Au microflowers (Ag_2S-Au MFs) and Au particles decorated AgAuS microsheets (Au-AgAuS MSs) by one-pot solvothermal method. These microstructures were used as SERS substrates for the detection of DEHA and DEHP. The LODs for SERS with Ag_2S-Au MFs substrate for DEHP and DEHA in orange juice reached 0.9×10^{-9} and 0.9×10^{-7} mol/L, respectively. Hu *et al.* [213] produced plasmonic bimetallic Au@Ag core-shell nanocubes (composed of a gold nanorod core and a silver cuboid shell) that can produce a richer and wider plasmonic resonance pattern than the gold nanocubes. The Au@Ag NCs-aggregated SERS platform possessed high sensitivity and repeatability, and the LODs of BBP and DEHP both reached 10^{-9} mol/L, which can realize rapid and sensitive label-free detection of phthalates in liquor samples. Wang *et al.* [214] also fabricated bimetallic SERs substrates (plasmonic core–shell Au nanospheres@Ag nanocubes (AuNS@AgNCs)) by liquid-liquid self-assembly method for rapid and sensitive detection of butyl benzyl phthalate in liquor samples. Their results showed that the plasma core-shell AuNS@AgNCs often exhibit richer localized surface plasmon resonance (LSPR) than AuNS.

However, the hydrophobicity of phthalates leads to its low affinity with substrates, which is still a challenge for the sensitive SERS detection of phthalates. To solve this problem, Xiang *et al.* [215] synthesized core-shell Au@Ag nanoparticles (NPs) stabilized inositol hexaphosphate (IP6) (denoted as Au@Ag@IP6), and then the Au@Ag@IP6 NPs were functionalized with 1-dodecanethiol (DT) to improve the loading of DEHP, to further improve the sensitivity of DEHP detection in food, with LODs of 10^{-8} mol/L. Liu *et al.* [216] used AuNP array self-assembly at liquid/liquid interface to detect BBP in liquors. By this method, the analyte was located in the nanogap of AuNP array, thereby increasing the affinity between BBP and substrate surface, and thereby the SERS sensitivity was improved accordingly.

Due to sample enrichment function of magnetic substrate, its combination with Raman enhancement substrate has also been widely concerned in trace detection. Aarthi *et al.* [217] confirmed that silver-modified Fe_3O_4 nanoparticles with magnetic separation function can be used as SERS active substrate to detect PAEs in landfill leachate near aquifers. Moreover, An *et al.* [218] synthesized a super-paramagnetic behavior and high sensitivity Fe_3O_4@C@Ag composite microspheres and used it as enhanced substrate for SERS detection of DEHP. The magnetic enrichment of Fe_3O_4@C@Ag

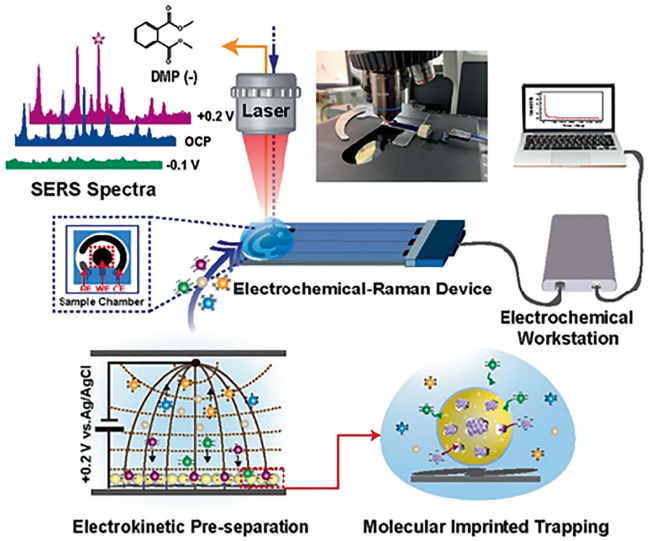

Fig. 8. Schematic lllustration of electro kinetic pre-separation and molecularly imprinted trapping of charged PAEs on a portable interface for selective SERS recognition. Reproduced with permission [222]. Copyright 2020, American Chemical Society.

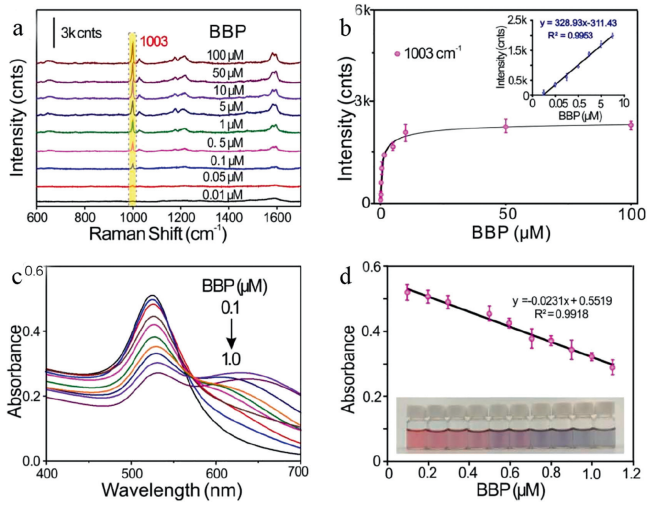

Fig. 9. (a) SERS spectra of BBP in different concentrations range from 0.01 μmol/L to 100 μmol/L. (b) SERS intensities at 1003 cm^{-1}. Each data point represents the intensity value from five SERS spectra. Error bars show the standard deviations. (c) UV–vis absorption spectra of the AuNPs@β-CD generated in the presence of various concentrations (0.1, 0.2, 0.3, 0.4, 0.5, 0.6, 0.7, 0.8, 0.9, and 1.0 μmol/L) of BBP. (d) The dependence intensity of the AuNPs@β-CD on the increasing concentrations of BBP (inset: corresponding photographs). Reproduced with permission [223]. Copyright 2019, American Chemical Society.

microspheres can effectively increase the concentration of the analyte to the region that can be sampled by the laser beam, thus enhancing the signal received by the detector. The detector signal was thus enhanced to realize the rapid SERS detection of DEHP with assistance from magnetic enrichment, and the detection limit reached 10^{-12} mol/L. Zhou *et al.* [219] modified Ag@Fe_3O_4@Ag with β-cyclodextrin, and the synthesized Ag@Fe_3O_4@Ag/β-cyclodextrin nanoparticles were used as SERS active substrate to detect BBP in liquor. After the hydrophobic BBP molecule was accurately captured by β-cyclodextrin in the substrate, the presence of Fe_3O_4 in the substrate under the influence of external magnetic field made the nanoparticles to rapidly gather (thus gathering BBP), which made the detection limit for the BBP substrate low enough.

To improve the sensitivity and selectivity of SERS sensor, Tu *et al.* [220] prepared a SERS aptasensor for rapid detection of trace DEHP. Firstly, silica was used to coat the silver nanoparticle clusters conjugated with Raman reporter molecules. As a protective shell, silica could prevent the dissociation of RRM and inhibit additional molecules from being adsorbed on the surface of metal nanostructures, thus providing high-intensity and stable SERS signals. Then, the SERS silica particles are functionalized by DEHP analogous molecules. High affinity SERS silica particles compete with DEHP molecules in the presence of DEHP samples, to bind with the aptamer on the magnetic particle. The concentration of DEHP in the sample was quantitatively determined *via* measuring of signal from free SERS silica particles in the supernatant after magnetic separation. The developed DEHP aptamer sensor had a detection limit of 8×10^{-12} mol/L and exhibited high selectivity and sensitivity.

To perfect the non-specific binding and weak spectral recognition defects of SERS detection, Yang *et al.* [221] prepared AuNP/PDA-MIP nanocomposite (NPs) by molecular imprinting technology. Thanks to the "hot spot" generated by AuNP and the recognition site generated by MIP, the composite material could be used as an excellent SERS substrate to achieve selective enrichment and recognition of dimethyl phthalate (DMP). The detection limit is as low as 1.0×10^{-10} mol/L. Later, Yang *et al.* [222] take advantage of electro kinetic preseparation (EP) and MIP technology to capture and selectively enrich PAEs and realized the label-free detection of charged PAEs molecules, as shown in Fig. 8. Similarly, AuNP/PDA-MIP NPs controllably synthesized provide “hot spots” and specific recognition site at the junction of NPs. Due to the introduction of an electric field, electrostatic attraction enables autonomous exclusion and separation of the similarly charged molecules as same as attraction and concentration of the oppositely charged molecules. Subsequently, targets are allowed selective adsorption by MIP cavities without the interference of analogues. The label-free SERS sensor based on multiple coupling separation, trapping, and enrichment strategies was demonstrated to detect charged phthalate plasticizers in real samples, and the detection limits of DMP and DEHP were as low as 2.7×10^{-12} mol/L and 2.3×10^{-11} mol/L, respectively.

To further improve the sensitivity and selectivity of phthalate plasticizers, some dual-mode sensors based on colorimetric (or fluorescence)/SERS have been developed. Li *et al.* [223] exploited a facile and sensitive colorimetric/SERS dual-mode sensor by constructing β-cyclodextrin (β-CD) stabilized AuNPs (AuNP@β-CD) colloid for BBP detection, which took the advantage of color changes and Raman scattering altering during the aggregated process of AuNP@β-CD. Due to AuNPs@β-CD larger specific surface and plentiful voids, their “aggregates” offer large-volume hot spots. The AuNPs@β-CD could capture hydrophobic groups of BBP by the hydrophobic cavities of β-CD units. The abundant hot spots of AuNPs@β-CD clusters triggered BBP are able to amplify the corresponding SERS signals, BBP detection limit is 0.01 μmol/L. In the colorimetric analysis of detecting BBP, AuNPs@β-CD clusters act as naked-eye indicators, and the colorimetric distinguishable response can be accurately quantified *via* UV–vis spectroscopy with a lowest detection limit of 14.9 nmol/L, as shown in Fig. 9.

Rong *et al.* [224] combined fluorescence analysis and SERS technology to prepare a dual-signal detection platform for DBP detection, as shown in Fig. 10. In this system, upconversion nanoparticles (UCNPs) decorated with gold nanoparticles (AuNPs) provide fluorescence signals and serve as Raman enhanced substrates, the aptamer was applied as an identification tag for PAEs. The bimodal nanosensor based on upconversion and SERS technology has been successfully developed for DBP detection in food and its packaging. The method had a good linear relationship, and the detection limits of fluorescence method and SERS method were 0.0087 ng/mL and 0.0108 ng/mL, respectively. Compared with the single-mode

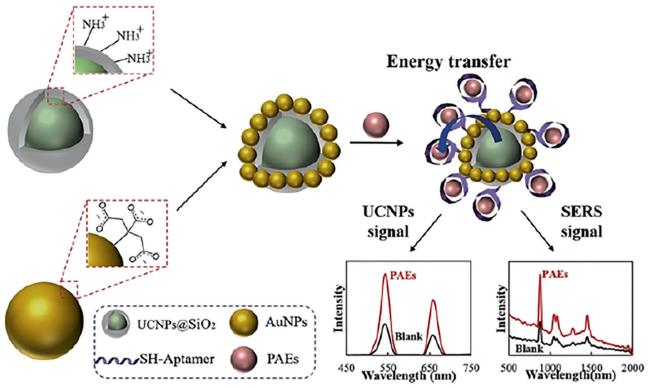

Fig. 10. Schematic illustration of fluorescence and SERS bimodal nanosensor for PAEs. Inset: the groups on the surface and the TEM images of nanoparticles. Changes in upconversion emission and Raman spectroscopy are also shown in their corresponding spectra and photos. Reproduced with permission [224]. Copyright 2021, Elsevier.

optical probe, the hybrid optical probe can exhibit multiple output signals and verify each other to ensure accuracy and prevent non-positive signals. And that bimodal probes have a wider detection range, lower sensitivity, outstanding reproducibility, excellent specificity and selectivity.

In conclusion, great progress has been achieved in the detection of PAEs by SERS technology, but there is still work to be done. For instance, the study on SERS signal enhancement mechanism lags behind relatively and needs to be strengthened, and more SERS substrate materials with good performance and low cost need to be developed. The SERS should be combined with MIP, aptamer and other technologies to achieve high specificity and sensitivity PAEs detection as reviewed and discussed herein.

3. Summary and perspectives

The detection of PAEs residues acting as one of the largest endocrine disruptors has attracted a great attention from all walks of life. However, due to their wide range of applications, wide variety of analogs, undiscovered harmful effects, and the need for effective analysis of environmental samples, they are still the current and different research topics in analytical chemistry. This paper mainly reviewed the research progress in the electrochemical and optical sensor detection of phthalates in the past decade and present. Various sensitivity-enhancement techniques for these biosensors have been developed [225–227], and the sensors showed a wide detection range and reduced the detection limit for PAEs detection. In particular, the designing strategies of sensors based on nanomaterials for PAEs detection even provide signal amplified with several orders of magnitude due to the accelerated signal transduction through a synergic effect among catalytic activity, conductivity, and compatibility. However, for exact diagnosis of trace PAEs residues, we still have much work to do to study sensors with higher sensitivity, higher specificity, and simpler portability. For instance, (1) design and synthesize new, efficient, stable, and environmentally friendly nanomaterials to provide more material sources for building high-performance sensors; (2) developing diversified and integrated detection devices, reducing detection costs, and improving the portability of on-site detection; (3) developing internal reference detection system and signal amplification detection platform to improve the accuracy and sensitivity of detection.

From another perspective of environmental protection and human health maintenance, human beings should reduce the use of plasticizers, and find low-toxic or even nontoxic and harmless plasticizer alternatives, and replace them with most commonly used PAEs such as DEHP and DBP at this stage.

Declaration of competing interest

The authors declare no competing financial interest.

Acknowledgments

This work was financially supported by the National Natural Science Foundation of China (Nos. 61871180, 61971187, and 61901168), Hunan Provincial Innovation Foundation for Postgraduate (No. CX20211074) and Open Funding of State Key Laboratory of Oral Diseases (No. SKLOD2022OF05).

References

[1] Y.M. Lee, J.E. Lee, W. Choe, et al., Environ. Int. 126 (2019) 635–643.
[2] J.L. Yang, Y.X. Li, Y. Wang, et al., TrAC-Trend. Anal. Chem. 72 (2015) 10–26.
[3] R.Y. Sun, H.S. Zhuang, Food Anal. Methods 8 (2015) 1990–1999.
[4] M. Negev, T. Berman, S. Reicher, et al., Chemosphere 192 (2018) 217–224.
[5] E. Fasano, F. Bono-Blay, T. Cirillo, et al., Food Control 27 (2012) 132–138.
[6] M. Jeddi, N. Rastkari, R. Ahmadkhaniha, M. Yunesian, Food Res. Int. 69 (2015) 256–265.
[7] C.Y. Chen, A.V. Ghule, W.Y. Chen, et al., Appl. Surf. Sci. 231-232 (2004) 447–451.
[8] D. Gao, Z. Li, H. Wang, H. Liang, Sci. Total Environ. 645 (2018) 1400–1409.
[9] X. Zheng, B.T. Zhang, Y. Teng, Sci. Total Environ. 476-477 (2014) 107–113.
[10] K.K. Selvaraj, G. Sundaramoorthy, P.K. Ravichandran, et al., Environ. Geochem. Health 37 (2015) 83–96.
[11] S. Orecchio, R. Indelicato, S. Barreca, J. Toxicol. Env. Heal. A 78 (2015) 1008–1018.
[12] I. Ustun, S. Sungur, R. Okur, et al., Food Anal. Methods 8 (2014) 222–228.
[13] V. Lo Turco, G. Di Bella, A.G. Potortì, et al., Eur. Food Res. Technol. 240 (2014) 451–458.
[14] T. Li, P.H. Yin, L. Zhao, et al., Water Sci. Technol. 71 (2015) 183–190.
[15] S. Sampath, K.K. Selvaraj, G. Shanmugam, et al., Environ. Pollut. 221 (2017) 407–417.
[16] M. Shi, Y.Y. Sun, Z.H. Wang, et al., Environ. Pollut. 250 (2019) 1–7.
[17] N. Alkan, A. Alkan, J. Castro-Jimenez, et al., Sci. Total Environ. 760 (2021) 143412.
[18] L.L. Zhang, J.L. Liu, H.Y. Liu, et al., Ecotoxicology 24 (2015) 967–984.
[19] T.C. Li, Y.C. Fan, D.S. Cun, et al., Front. Environ. Sci. Eng. 14 (2020) 139–149.
[20] R.L. Li, J.B. Liang, Z.B. Gong, et al., Sci. Total Environ. 580 (2017) 388–397.
[21] Y. Ait Bamai, C. Miyashita, A. Araki, et al., Sci. Total Environ. 618 (2018) 1408–1415.
[22] G. Zaki, T. Shoeib, Sci. Total Environ. 618 (2018) 142–150.
[23] Q. Yang, Z.D.Wen X.L.Huang, et al., J. Great. Lakes Res. 47 (2021) 437–446.
[24] A. Paluselli, V. Fauvelle, N. Schmidt, et al., Sci. Total Environ. 621 (2018) 578–587.
[25] W. Zhang, X. Li, C. Guo, J. Xu, Environ. Sci. Pollut. Res. 28 (2021) 25207–25217.
[26] Y. Xu, Z.G. Song, X.P. Chang, et al., Ecotoxicol. Environ. Saf. 208 (2021) 111624.
[27] Z.P. Cheng, Y. Wang, B.T. Qiao, et al., Sci. Total Environ. 768 (2021) 144945.
[28] X.Y. Gao, J. Li, X.N. Wang, et al., Ecotoxicol. Environ. Saf. 171 (2019) 564–570.
[29] M.M. Abdel daiem, J. Rivera-Utrilla, R. Ocampo-Perez, et al., J. Environ. Manage. 109 (2012) 164–178.
[30] X.T. Liu, C.F. Peng, Y.M. Shi, et al., Environ. Sci. Technol. 53 (2019) 1675–11683.
[31] D. Kim, J.H. Kim, S.C. Seo, Sustainability 12 (2020) 6166.
[32] L.Y. Wang, Y.Y. Gu, Z.M. Zhang, et al., Sci. Total Environ. 770 (2021) 144705.
[33] Q.Y. Zou, S.L. Hong, H.Y. Kang, et al., Sci. Rep. 10 (2020) 14625.
[34] M. Minatoya, A. Araki, C. Miyashita, et al., Sci. Total Environ. 579 (2017) 606–611.
[35] H. Q.Anh, H.M. N.Nguyen, T.Q. Do, et al., Sci. Total Environ. 760 (2021) 143380.
[36] A.K. Wesselink, V. Fruh, R. Hauser, et al., J. Expo. Sci. Env. Epidl. 31 (2021) 461–475.
[37] S.S. Yalcin, I. Erdal, S. Cetinkaya, B. Oguz, Int. J. Environ. Health Res. 31 (2021) 1–14.
[38] D. Salazar-Beltrán, L. Hinojosa-Reyes, E. Ruiz-Ruiz, et al., Food Anal. Methods 11 (2017) 48–61.
[39] H.J. Heo, M.J. Choi, J.K. Park, et al., Water 12 (2019) 122.
[40] X. Li, W.P. Zhang, J.P. Lv, et al., Environ. Sci. Eur. 33 (2021) 19.
[41] B. Prasad, Environ. Sci.: Proc. Imp. 23 (2021) 389–399.
[42] X.G. Zhao, H.Y. Jin, D.H. Li, et al., Mar. Pollut. Bull. 160 (2020) 111667.
[43] D.C. Wu, X.L. Chen, F. Liu, et al., Microchem. J. 159 (2020) 105563.
[44] H. Chen, W. Mao, Y.Q. Shen, et al., Environ. Sci. Pollut. Res. 26 (2019) 24609–24619.
[45] S. Singh, S.S. Li, Int. J. Mol. Sci. 13 (2012) 10143–10153.
[46] Q.Y. Shi, J.C. Tang, L. Wang, et al., Ecotoxicol. Environ. Saf. 213 (2021) 112041.
[47] J. Chi, H.T. Zhang, D.X. Zhao, Mar. Pollut. Bull. 162 (2021) 111881.
[48] A. Ranjbar Jafarabadi, M. Dashtbozorg, E. Raudonyte-Svirbutaviciene, et al., Sci. Total Environ. 775 (2021) 145822.

[49] G. Bolat, Y.T. Yaman, S. Abaci, Sens. Actuators B: Chem. 299 (2019) 127000.
[50] A. Estevez-Danta, R. Rodil, B. Perez-Castano, et al., Talanta 224 (2021) 121912.
[51] N. Yue, C. Deng, C.M. Li, et al., J. Agr. Food Chem. 68 (2020) 6910–6918.
[52] Y. Kudo, K. Obayashi, H. Yanagisawa, et al., J. Chromatogra. A 1602 (2019) 441–449.
[53] S. Keresztes, E. Tatar, Z. Czegeny, et al., Sci. Total Environ. 458-460 (2013) 451–458.
[54] O.H. Fred-Ahmadu, O.O. Ayejuyo, N.U. Benson, Data Brief 31 (2020) 105755.
[55] R.Y. Sun, H.S. Zhuang, Anal. Biochem. 480 (2015) 49–57.
[56] R. Cariou, F. Larvor, F. Monteau, et al., Food Chem. 196 (2016) 211–219.
[57] Y. Liu, Y.X. Lai, G.J. Yang, et al., J. Biomed. Nanotechnol. 13 (2017) 1253–1259.
[58] H. Shi, T. Jin, J.W. Zhang, et al., Chin. Chem. Lett. 31 (2020) 155–158.
[59] Y.J. Tang, Z.Y. Li, N.Y. He, et al., J. Biomed. Nanotechnol. 9 (2013) 312–317.
[60] Y. Liu, Y. Deng, H.M. Dong, et al., Sci. China Chem. 60 (2017) 329–337.
[61] L. He, H.W. Yang, P.F. Xiao, et al., J. Biomed. Nanotechnol. 13 (2017) 1243–1252.
[62] M. Liu, A. Khan, Z.F. Wang, et al., Biosens. Bioelectron. 130 (2019) 174–184.
[63] N. Jaffrezic-Renault, J. Kou, D. Tan, Z.Z. Guo, Anal. Bioanal. Chem. 412 (2020) 5913–5923.
[64] X.B. Mou, Z. Chen, T.T. Li, et al., J. Biomed. Nanotechnol. 15 (2019) 1832–1838.
[65] S.I. Kaya, A. Cetinkaya, N. K.Bakirhan, S.A. Ozkan, Trends Environ. Anal. Chem. 28 (2020) e100106.
[66] Z.Y. Li, J.H. Wang, H.W. Yang, et al., J. Biomed. Nanotechnol. 13 (2017) 1272–1280.
[67] H. Xie, K.L. Di, R.R. Huang, et al., Chin. Chem. Lett. 31 (2020) 1737–1745.
[68] H.W. Yang, W.B. Liang, J. Si, et al., J. Biomed. Nanotechnol. 10 (2014) 3610–3619.
[69] C.L. Tang, Z.Y. He, H.M. Liu, et al., J. Nanobiotechnol. 18 (2020) 62.
[70] Y. Deng, W. Wang, C. Ma, Z.Y. Li, J. Biomed. Nanotechnol. 9 (2013) 1378–1382.
[71] G.J. Yang, Y.X. Lai, Z.Q. Xiao, et al., Chin. Chem. Lett. 29 (2018) 1857–1860.
[72] Y. Deng, W. Wang, L.M. Zhang, et al., J. Biomed. Nanotechnol. 9 (2013) 318–321.
[73] J. Liu, S.A. Dong, Q.G. He, et al., Biomolecules 9 (2019) 245.
[74] Y.X. Lai, L.J. Wang, Y. Liu, et al., J. Biomed. Nanotechnol. 14 (2018) 44–65.
[75] W. Wang, Y. Deng, S. Li, et al., J. Biomed. Nanotechnol. 9 (2013) 736–740.
[76] Y.H. Zhang, Y.N. Lei, H. Lu, et al., Food Chem. 346 (2021) 128895.
[77] Y. Liu, T.T. Li, C.X. Ling, et al., Chin. Chem. Lett. 30 (2019) 2211–2215.
[78] X.Z. Feng, X.R. Su, A. Ferranco, et al., J. Biomed. Nanotechnol. 16 (2020) 29–39.
[79] Q. Wang, Q. Xue, T. Chen, et al., Chin. Chem. Lett. 32 (2021) 609–619.
[80] Q.G. He, J. Liu, X.P. Liu, et al., Colloids Surf. B 172 (2018) 565–572.
[81] Q.G. He, Y.L. Tian, Y.Y. Wu, et al., Biomolecules 9 (2019) 176.
[82] G.J. Yang, H. Huang, Z.Q. Xiao, et al., J. Biomed. Nanotechnol. 16 (2020) 548–552.
[83] A. Khanmohammadi, A.J. Ghazizadeh, P. Hashemi, et al., J. Iran. Chem. Soc. 17 (2020) 2429–2447.
[84] Z.Y. Xu, X.X. Jiang, S.P. Liu, M.H. Yang, Chin. Chem. Lett. 31 (2020) 185–188.
[85] Y. Liu, Y. Deng, T.T. Li, et al., J. Biomed. Nanotechnol. 14 (2018) 2156–2161.
[86] Z.X. Shi, G.K. Li, Y.F. Hu, Chin. Chem. Lett. 30 (2019) 1600–1606.
[87] Q.G. He, J. Liu, X.P. Liu, et al., Electrochim. Acta 296 (2019) 683–692.
[88] Y.L. Fang, H.R. Liu, Y. Wang, et al., J. Biomed. Nanotechnol. 17 (2021) 407–415.
[89] H. Chen, Y.Q. Wu, Z. Chen, et al., J. Biomed. Nanotechnol. 13 (2017) 1619–1630.
[90] Q.K. Zeng, X.L. Qi, M.Y. Zhang, et al., Int J. Biol. Macromol. 145 (2020) 1049–1058.
[91] J. Fu, Z. Dang, Y. Deng, et al., J. Biomed. Nanotechnol. 8 (2012) 669–675.
[92] Z.L. Ding, Y.L. Wang, Q. Zhou, et al., Biomolecules 10 (2019) 68.
[93] F. Li, Z.F. Wang, Y.F. Huang, et al., J. Biomed. Nanotechnol. 11 (2015) 1776–1782.
[94] M.A.A. Shah, N.Y. He, Z.Y. Li, et al., J. Biomed. Nanotechnol. 10 (2014) 2332–2349.
[95] Y.Y. Wu, P.H. Deng, Y.L. Tian, et al., J. Nanobiotechnol. 18 (2020) 112.
[96] F. Magesa, Y.Y. Wu, S.A. Dong, et al., Biomolecules 10 (2020) 110.
[97] Y.J. Li, H.P. Dai, N.N. Feng, et al., Mater. Express. 9 (2019) 59–64.
[98] H.W. Yang, M. Liu, H.R. Jiang, et al., J. Biomed. Nanotechnol. 13 (2017) 655–664.
[99] L.M. Zhang, K. Xia, Y.Y. Bai, et al., J. Biomed. Nanotechnol. 10 (2014) 1440–1449.
[100] Y.X. Liu, S. Zhang, X. Ren, et al., RSC Adv. 5 (2015) 57346–57353.
[101] A.I. Zia, A.R.M. Syaifudin, S.C. Mukhopadhyay, et al., J. Phys. Conf. Ser. 439 (2013) 012026.
[102] Y.R. Liang, Z.M. Zhang, Z.J. Liu, et al., Biosens. Bioelectron. 91 (2017) 199–202.
[103] B.S. He, J.W. Li, Rare Met. 40 (2021) 1099–1109.
[104] L.J. Xu, J.J. Du, Y. Deng, et al., J. Biomed. Nanotechnol. 8 (2012) 1006–1011.
[105] X.J. Li, J.F. Ping, Y.B. Ying, TrAC-Trend. Anal. Chem. 113 (2019) 1–12.
[106] S.Q. Xiong, J.J. Cheng, L.L. He, et al., Anal. Methods 6 (2014) 1736–1742.
[107] S.Q. Xiong, J.J. Cheng, L.L. He, et al., J. Electroanal. Chem. 743 (2015) 18–24.
[108] F.J. Xiao, M.Y. Guo, J.Z. Wang, et al., Anal. Chim. Acta 1043 (2018) 35–44.
[109] F.J. Xiao, X.R. Yan, H.L. Li, et al., Sens. Actuators B: Chem. 288 (2019) 476–485.
[110] X.Y. Jiang, Y.Q. Xie, D.J. Wan, et al., Sensors 20 (2020) 901.
[111] J. Annamalai, N. Vasudevan, et al., Anal. Chim. Acta 1135 (2020) 175–186.
[112] J.W. Li, H.L. Jin, M. Wei, et al., Sens. Actuators B: Chem. 331 (2021) 129401.
[113] Y.X. Lai, C.X. Zhang, Y. Deng, et al., Chin. Chem. Lett. 30 (2019) 160–162.
[114] Y.Y. Wu, P.H. Deng, Y.L. Tian, et al., Bioelectrochemistry 131 (2020) 107393.
[115] Y.L. Tian, P.H. Deng, Y.Y. Wu, et al., Biomolecules 9 (2019) 294.
[116] Y.X. Lai, Y. Deng, G.J. Yang, et al., J. Biomed. Nanotechnol. 14 (2018) 1688–1694.
[117] D.R. Kumar, G. Dhakal, V.Q. Nguyen, J.J. Shim, Anal. Chim. Acta 1141 (2021) 71–82.
[118] J. Wackerlig, R. Schirhagl, Anal. Chem. 88 (2016) 250–261.
[119] T. Wu, X.P. Wei, X.H. Ma, J.P. Li, Microchim. Acta 184 (2017) 2901–2907.
[120] X.Q. Li, L. Zhong, R.L. Liu, et al., Microchim. Acta 186 (2019) 688.
[121] M. Panagiotopoulou, S. Kunath, P.X. Medina-Rangel, et al., Biosens. Bioelectron. 88 (2017) 85–93.
[122] J.J. BelBruno, Chem. Rev. 119 (2019) 94–119.
[123] M. Yoshikawa, K. Tharpa, S.O. Dima, Chem. Rev. 116 (2016) 11500–11528.
[124] A.I. Zia, S.C. Mukhopadhyay, P.L. Yu, et al., Biosens. Bioelectron. 67 (2015) 342–349.
[125] A. Adumitrăchioaie, M. Tertis, A. Cernat, et al., Int. J. Electrochem. Sci. 13 (2018) 2556–2576.
[126] R.G. Gui, H. Jin, H.J. Guo, Z.H. Wang, Biosens. Bioelectron. 100 (2018) 56–70.
[127] J. He, R.H. Lv, J. Zhu, K. Lu, Anal, Chim. Acta 661 (2010) 215–221.
[128] I. Tabushi, K. Kurihara, K. Naka, et al., Tetrahedron Lett. 28 (1987) 4299–4302.
[129] K. Haupt, P.X. Medina Rangel, B.T.S. Bui, Chem. Rev. 120 (2020) 9554–9582.
[130] S. Venkatesh, C.C. Yeung, Q.J. Sun, et al., Sens. Actuators B: Chem. 259 (2018) 650–657.
[131] X. Zhao, X. Ju, S. Qiu, et al., Russ. J. Electrochem. 54 (2018) 636–643.
[132] Z.H. Zhang, L.J. Luo, R. Cai, H.J. Chen, Biosens. Bioelectron. 49 (2013) 367–373.
[133] Y. Li, J.J. Kang, X.Y. Zhao, et al., Chem. J. Chin. Univ. 40 (2019) 448–455.
[134] Q.T. Zhou, M. Guo, S.C. Wu, et al., J. Electroanal. Chem. 897 (2021) 115549.
[135] L. Li, L.L. Yang, Z.L. Xing, et al., Analyst 138 (2013) 6962–6968.
[136] C.X. Lu, Z.G. Tang, X.X. Gao, et al., Microchim. Acta 185 (2018) 373.
[137] L.X. Chen, S.F. Xu, J. H.Li, Chem. Soc. Rev. 40 (2011) 2922–2942.
[138] T. Fan, W.M. Yang, N.W. Wang, et al., J. Appl. Polym. Sci. 133 (2016) 43484.
[139] W.Z. Xu, X.M. Zhang, W.H. Huang, et al., Appl. Surf. Sci. 426 (2017) 1075–1083.
[140] X.J. Li, X.J. Wang, L.L. Li, et al., Talanta 131 (2015) 354–360.
[141] Q.W. Chen, C. Yuan, C.Y. Zhai, et al., Chin. Chem. Lett. 33 (2022) 983–986.
[142] P.W. Gao, Y.Z. Shen, C. Ma, et al., Analyst 146 (2021) 6178.
[143] Y.J. Tang, H.N. Liu, H. Chen, et al., J. Biomed. Nanotechnol. 16 (2020) 763–788.
[144] L. He, R.R. Huang, P.F. Xiao, et al., Chin. Chem. Lett. 32 (2021) 1593–1602.
[145] W.F. Guo, C.X. Zhang, T.T. Ma, et al., J. Nanobiotechnol. 19 (2021) 166.
[146] X.B. Mou, D.N. Sheng, Z. Chen, et al., J. Biomed. Nanotechnol. 15 (2019) 2393–2400.
[147] R.R. Huang, Z.S. Chen, M. Liu, et al., Sci. China Chem. 60 (2017) 786–792.
[148] G.J. Yang, Y. Liu, Y. Deng, et al., J. Biomed. Nanotechnol. 17 (2021) 2240–2246.
[149] X.B. Mou, T.T. Li, J.H. Wang, et al., J. Biomed. Nanotechnol. 11 (2015) 2057–2066.
[150] K. Ikebukuro, C. Kiyohara, K. Sode, Anal. Lett. 37 (2004) 2901–2909.
[151] M. Liu, L. Xi, T. Tan, et al., Chin. Chem. Lett. 32 (2021) 1726–1730.
[152] H.N. Liu, H.M. Dong, Z. Chen, et al., J. Biomed. Nanotechnol. 13 (2017) 1333–1343.
[153] M. Liu, X.C. Yu, Z. Chen, et al., J. Nanobiotechnol. 15 (2017) 81.
[154] C. Ma, C.Y. Li, F. Wang, et al., J. Biomed. Nanotechnol. 9 (2013) 703–709.
[155] S.I. Kaya, A. Cetinkaya, S.A. Ozkan, Crit. Rev. Anal. Chem. 51 (2021) 1–21.
[156] Z.M. Li, Y. Yu, Z.L. Li, T. Wu, Anal. Bioanal. Chem. 407 (2015) 2711–2726.
[157] A.S. Sadeghi, N. Ansari, M. Ramezani, et al., Biosens. Bioelectron. 118 (2018) 137–152.
[158] Z. Li, M.A. Mohamed, A.M. Vinu Mohan, et al., Sensors 19 (2019) 5435.
[159] Y. Han, D.L. Diao, Z.W. Lu, et al., Anal. Chem. 89 (2017) 5270–5277.
[160] X. Wu, D.L. Diao, Z.W. Lu, et al., JoVE-J. Vis. Exp. 133 (2018) 56814.
[161] Q. Lu, X.X. Liu, J.J. Hou, et al., Molecules 25 (2020) 747.
[162] Y.Z. Shen, J. Guan, C. Ma, et al., Anal. Chem. 94 (2022) 1742–1751.
[163] L.B. Nie, F.H. Liu, P. Ma, X.Y. Xiao, J. Biomed. Nanotechnol. 10 (2014) 2700–2721.
[164] Y. Liu, T.T. Li, C.X. Ling, et al., Chin. Chem. Lett. 30 (2019) 2359–2362.
[165] L. Gong, L. Zhao, M.D. Tan, et al., J. Biomed. Nanotechnol. 17 (2021) 509–528.
[166] N. Yan, J.L. Song, F.Y. Wang, et al., Chin. Chem. Lett. 30 (2019) 1984–1988.
[167] Z.Y. He, Z.R. Tong, B.Y. Tan, et al., J. Biomed. Nanotechnol. 17 (2021) 1364–1370.
[168] H.L. Zhang, P.F. Xu, X.T. Zhang, et al., Chin. Chem. Lett. 31 (2020) 1083–1086.
[169] H.M. Hu, L.L. Fan, X.J. Li, et al., J. Pharmaceut. Biomed. 75 (2013) 123–129.
[170] S. Li, H.N. Liu, Y.Y. Jia, et al., J. Biomed. Nanotechnol. 9 (2013) 689–698.
[171] B. Liu, Y.Y. Jia, M. Ma, et al., J. Biomed. Nanotechnol. 9 (2013) 247–256.
[172] H. Yanagisawa, S. Fujimaki, Anal. Sci. 35 (2019) 1215–1219.
[173] B.J. Johnson, A.P. Malanoski, J.S. Erickson, Sensors 20 (2020) 5857.
[174] R. Bala, R.K. Sharma, N. Wangoo, Anal. Bioanal. Chem. 408 (2016) 333–338.
[175] K. Akshaya, C. Arthi, A.J. Pavithra, et al., Photodiagn. Photodyn. 30 (2020) 101699.
[176] S. Sun, S.H. Qian, J.P. Zheng, et al., Analyst 145 (2020) 6968–6973.
[177] H. Ahmadi, S. Keshipour, F. Ahour, Sci. Rep. 10 (2020) 14185.
[178] L.H. Wu, S.L. Yao, H. Xu, et al., Chin. Chem. Lett. 33 (2022) 541–546.
[179] J.X. Zhao, Z.W. Lu, S. Wang, et al., Anal. Chem. 93 (2021) 4317–4325.
[180] Y. Liu, G.J. Yang, T.T. Li, et al., Chin. Chem. Lett. 32 (2021) 1957–1962.
[181] R.H. Guo, C.C. Shu, K.J. Chuang, G.B. Hong, Mater. Lett. 293 (2021) 129756.
[182] Y.M. Yan, Y. Qu, R. Du, et al., Anal. Methods 13 (2021) 5179.
[183] Y.T. Qin, Y. Wan, J. Guo, M.T. Zhao, Chin. Chem. Lett. 33 (2022) 693–702.
[184] N.F. Zhu, Y.M. Zou, M.L. Huang, et al., Talanta 186 (2018) 104–109.
[185] Z.W. Qiu, Y.T. Xue, J.Y. Li, et al., Chin. Chem. Lett. 32 (2021) 2807–2811.
[186] M. Zhang, Y.Q. Liu, B.C. Ye, Chem. Commun. 47 (2011) 11849–11851.
[187] D. Seol, D. Jang, J.W. Oh, et al., Environ. Res. 170 (2019) 238–242.
[188] Y.F. Kang, L. Zhang, Q.H. Lai, et al., Polym-Plast. Tech. Mat. 60 (2021) 60–69.
[189] T.T. Li, H. Yi, Y. Liu, et al., J. Biomed. Nanotechnol. 14 (2018) 150–160.
[190] L. Yu, Y.M. Qiao, L.X. Miao, et al., Chin. Chem. Lett. 29 (2018) 1545–1559.

[191] J.Y. Lu, J.X. Wang, Y. Li, et al., Sens. Actuators B: Chem. 331 (2021) 129396.
[192] H.R. Jiang, X. Zeng, Z.J. Xi, et al., J. Biomed. Nanotechnol. 9 (2013) 674–684.
[193] D.R. Cao, H. Meier, Chin. Chem. Lett. 30 (2019) 1758–1766.
[194] W. Wei, J. Wang, C.B. Tian, et al., Analyst 143 (2018) 5481–5486.
[195] J.M. Yan, Y.N. Lu, S.W. Xie, et al., J. Biomed. Nanotechnol. 17 (2021) 312–321.
[196] T. Li, Z.K. Gao, N.W. Wang, et al., RSC Adv. 6 (2016) 54615–54622.
[197] S. Chen, J.L. Fu, S. Zhou, et al., Food Chem. 367 (2022) 130505.
[198] W.Z. Xu, T. Li, W.H. Huang, et al., RSC Adv. 7 (2017) 51632–51639.
[199] Y.Y. Wang, Z.P. Zhou, W.Z. Xu, et al., Polym. Int. 67 (2018) 1003–1010.
[200] Z.P. Zhou, T. Li, W.Z. Xu, et al., Sens. Actuators B: Chem. 240 (2017) 1114–1122.
[201] X.M. Wang, C. Chen, Y.F. Chen, et al., Food Agr. Immunol. 31 (2020) 813–826.
[202] Y.Y. Wang, W.T. Li, X.T. Hu, et al., Food Chem. 352 (2021) 129352.
[203] H.J. Lim, A.R. Kim, M.Y. Yoon, Biosens. Bioelectron. 121 (2018) 1–9.
[204] J. Dolai, H. Ali, N.R. Jana, New J. Chem. 45 (2021) 19088.
[205] C.K. Qiu, Y.J. Gong, Y.X. Guo, et al., Anal. Chem. 91 (2019) 13355–13359.
[206] B. Cromwell, M. Dubnicka, S. Dubrawski, et al., ACS Omega 4 (2019) 17009–17015.
[207] Y. Zhou, Z.F. Wang, Y.L. Peng, et al., J. Biomed. Nanotechnol. 17 (2021) 744–770.
[208] Y.S. Chen, S.L. Cheng, A.M. Zhang, et al., J. Biomed. Nanotechnol. 14 (2018) 1773–1784.
[209] J. Wang, Y.R. Zhou, Q.Q. Wang, et al., Chin. J. Anal. Chem. 48 (2020) 1625–1632.
[210] Z.W. Zuo, K. Zhu, L.X. Ning, et al., Appl. Surf. Sci. 325 (2015) 45–51.
[211] Y.P. Wu, W.F. Yu, B.H. Yang, P. Li, Analyst 143 (2018) 2363–2368.
[212] Q. Cao, R.C. Che, ACS Appl. Mater. Interfaces 6 (2014) 7020–7027.
[213] X.Y. Hu, X.R. Wang, Z.P. Ge, et al., Analyst 144 (2019) 3861–3869.
[214] Q.Q. Wang, J. Wang, M. Li, et al., Spectrochim. Acta A 248 (2021) 119131.
[215] Y. Xiang, M.H. Li, X.Y. Guo, et al., Sens. Actuators B: Chem. 262 (2018) 44–49.
[216] J.N. Liu, J.Y. Li, F. Li, et al., Anal. Bioanal. Chem. 410 (2018) 5277–5285.
[217] A. Aarthi, M. Umadevi, R. Parimaladevi, G.V. Sathe, J. Mol. Liq. 252 (2018) 97–102.
[218] Q. An, P. Zhang, J.M. Li, Nanoscale 4 (2012) 5210–5216.
[219] Y.R. Zhou, J.Y. Li, L. Zhang, et al., Anal. Bioanal. Chem. 411 (2019) 5691–5701.
[220] D.D. Tu, J.T. Garza, G.L. Cote, RSC Adv. 9 (2019) 2618–2625.
[221] Y.Y. Yang, Y.T. Li, X.J. Li, et al., Chem. Eng. J. 402 (2020) 125179.
[222] Y.Y. Yang, Y.T. Li, W.L. Zhai, et al., Anal. Chem. 93 (2021) 946–955.
[223] J.Y. Li, X.Y. Hu, Y.R. Zhou, et al., ACS Appl. Nano Mater. 2 (2019) 2743–2751.
[224] Y.W. Rong, S.J. Ali, Q. Ouyang, et al., J. Food Compos. Anal. 100 (2021) 103929.
[225] D.Q. Chen, X.Y. Sun, K.H. Zhang, et al., Sensors 17 (2017) 1681.
[226] M. Tang, Y.F. Wu, D.L. Deng, et al., Sens. Actuators B: Chem. 258 (2018) 304–312.
[227] S. Mohammadi, A.V. Nadaraja, D.J. Roberts, et al., Sens. Actuators A: Phys. 303 (2020) 111663.